Journal of Archaeological Science: Reports 33 (2020) 102508

Contents lists available at ScienceDirect

Journal of Archaeological Science: Reports

journal homepage: www.elsevier.com/locate/jasrep

# Investigating post-depositional sediment mixing at an archaeological site on the northern Plains using a portable optically stimulated luminescence (OSL) reader

Kennedy Munyikwa[a,*], Krista Gilliland[b], Evan Plumb[c], Terrance Gibson[b]

[a] Centre for Science, Athabasca University, 1 University Drive, Athabasca, Alberta T9S 3A3, Canada
[b] Western Heritage, 46A Riel Drive, St Albert, Alberta T8N 3Z8, Canada
[c] Earth and Atmospheric Science, University of Alberta, Edmonton, Alberta T6G 2E3, Canada

ARTICLE INFO

*Keywords:*
Portable OSL reader
Optically stimulated luminescence dating
Sediment mixing
Archaeological site
Great Plains
Aeolian
Stratigraphy

ABSTRACT

The Bodo Archaeological locality is a major multicomponent site located in east-central Alberta, Canada, in a fossil aeolian dune landscape. About five decades ago, oilfield-related pipeline construction activity resulted in the post-depositional stratigraphic disturbance of some parts of the site. However, the absence of easily discernible signs of anthropogenic disturbances makes visual identification of the disrupted sequences difficult. As a result, identifying sequences that yield accurate reconstructions of the archaeological occupations is problematic. In an effort to differentiate between areas at the site that are intact from those that have been disturbed, this study employed a portable optically stimulated luminescence reader to construct luminescence profiles that show the variation of luminescence signal intensities with depth. The results show that depositional sequences that have undisrupted stratigraphy display signal intensities that decrease up the sequence, correlable with depositional age. Conversely, areas with disrupted stratigraphy are characterized by signals that fluctuate with depth, which results from mixing of strata of dissimilar age. Luminescence profiling also allows the approximation of relative ages of depositional units and these show that, in the undisturbed sites, sediments at the base of the sequences are about three to four times older than sediments in the upper parts. Overall, the ability to identify stratigraphic sequences that are intact enables investigators to expend time and resources on stratigraphic records that yield accurate archaeological reconstructions.

## 1. Introduction

An enduring theme in the study of archaeological sites is the placement of constraints on the chronology of occupation of a site as well as the correlation of how environmental changes influence the timing of occupation. The accuracy of such reconstructions, however, ultimately hinges on two elements: that the stratigraphic sequence at the site be free from post-depositional sediment mixing, and that the depositional age associated with the occupation be ascertained using a competent dating method. It is within this broad framework that, in 2012, a historic resources impact assessment (HRIA) was embarked upon at the Bodo Archaeological Locality, which lies on the northwest margin of the North American Great Plains. The investigations were associated with oilfield pipeline installation and, during the assessment, it was discovered that some areas at the locality had been disrupted by earlier pipeline construction activities. To enable accurate archaeological reconstructions to be made, therefore, it was imperative to distinguish areas whose stratigraphic integrity had been disrupted. Accordingly, this study explored the ability of luminescence profiling using a portable optically stimulated luminescence (OSL) reader (e.g. Sanderson and Murphy, 2010) to identify parts of the site that had been affected by post-depositional anthropogenic disruptions from those that had remained intact. The Bodo Archaeological Locality shares some stratigraphic similarities with other archaeological sites on the Great Plains (e.g. Wood, 1998). Thus, if successfully applied, the methodology could also be employed at multiple other localities on the Great Plains as well as in other geologically suitable areas where post-depositional stratigraphic disturbances might have occurred during the late Quaternary.

The Great Plains, a region that covers the central plains of the United States and the Prairie provinces of Canada, features abundant surface deposits of aeolian origin (e.g. Arbogast, 1996; Forman et al., 2001; Holliday, 2001). Comprising dunes, sand sheets and loess, the aeolian deposits have been active at various times during the late Pleistocene and Holocene epochs. Stratigraphically, the depositional

* Corresponding author.
*E-mail address:* kenm@athabascau.ca (K. Munyikwa).

https://doi.org/10.1016/j.jasrep.2020.102508
Received 18 November 2019; Received in revised form 19 July 2020; Accepted 23 July 2020

sequences have been interpreted as indicative of environmental changes, with the aeolian deposits pointing to past episodes of enhanced aridity (e.g. Muhs and Holliday, 2001; Holliday, 2001; Forman et al., 2001; Hall et al., 2010; Hall and Goble, 2012; Halfen et al., 2015). However, moisture balance, sediment supply, and wind regime are also thought to play a role in the preservation of aeolian records (e.g. Stauch, 2019). In archaeological contexts, the timing of late Pleistocene and Holocene environmental changes on the Great Plains are important to human settlement patterns because ancestral Indigenous peoples are thought to have dispersed widely on the continent as the climate ameliorated sometime after the Last Glacial Maximum (LGM), which occurred ca. 20,000 years ago (e.g. Hetherington et al., 2004; Montenegro et al., 2006; Waters and Stafford, 2007; Geobel et al., 2008). Their initial arrival on the continent is thought to have occurred just before the LGM (e.g. Potter et al., 2018; Becerra-Valdivia and Higham, 2020).

Notably, multiple occupation sites that have been identified on the Great Plains show that humans had spread widely throughout the region by 11,000 years ago (Wood, 1998). Many of the archaeological finds occur stratigraphically intercalated within sequences of aeolian deposits (e.g. Hall and Goble, 2008; Holen, 1990; Holliday, 2000b; Wolfe et al., 2007; Hall, Miller and Goble, 2010, Munyikwa and Brown, 2014; Munyikwa et al., 2019). The close association between aeolian deposits and archaeological sites may be because the diverse ecosystems of aeolian landscapes attracted wildlife on which the humans subsisted (e.g. Running et al., 2002). The dune relief may have also offered protection from the elements for the inhabitants (Hamilton and Nicholson, 1999; Running et al., 2002). Additionally, the dune landscape may have been used for trapping bison, for example at the Casper Site in Wyoming (e.g. Frison, 2013), or at the Fincastle Site in Alberta (Bubel, 2014). The potential of the aeolian record lies in its applicability for luminescence dating to establish the timing of human settlement, and the insights gained into the palaeoenvironment. The record on human settlement would include the timing of the settlement and how it relates to local and regional environmental processes (e.g. Crumley, 1994; Feathers, 2003a; Adderley, et al., 2004; Balee, 2006). However, such reconstructions would only be accurate if the integrity of the site has not been compromised and if the dating is precise (Feathers, 2003a). The site integrity is largely governed by the degree of post-depositional disturbance that has taken place. Such disturbance can be the result of human activity. Alternatively, it can be due to natural processes, such as pedoturbation (e.g. freeze/thaw processes) or bioturbation (e.g. due to burrowing fauna, root action, or tree growth [Bateman et al., 2003, 2007; Leigh, 2001]).

For over 50 years, radiocarbon dating has been indispensable in constructing chronological frameworks at archaeological sites on the Great Plains (e.g. Neuman, 1967; Holliday, 2000a). Over the last three decades, however, optically stimulated luminescence (OSL) techniques have emerged as another useful dating technique, particularly at archaeological sites with poor organic preservation (e.g. Aitken, 1998; Roberts, 1997; Feathers, 2003a). Settlements in aeolian settings are particularly amenable to dating using OSL techniques because aeolian transport provides ample opportunities for the signal in the sediment to be zeroed before burial (Aitken, 1998; Lian and Roberts, 2006; Wintle, 2008). Furthermore, luminescence methods date the burial event itself, as opposed to events subsequent to the burial and, thus, provide data that are particularly useful for environmental reconstruction (Feathers, 2003a).

The luminescence properties of sediment that surround the artifact may also be used to determine whether post-depositional mixing has occurred at an archaeological site. One approach would be to collect closely spaced samples up the depositional sequence and then date them using OSL to see if the ages are in a stratigraphic order that is consistent with the principle of superposition (i.e. oldest at the bottom and youngest at the top). Alternatively, more advanced luminescence approaches such as single-grain dating procedures can be employed (Bøtter-Jensen et al., 2000; Lamothe and Auclair, 2000; Roberts et al., 2000; Feathers, 2003b; Bateman et al., 2007; Boulter et al., 2010). However, both these methods are time- and resource-intensive and beyond routine reconnaissance approaches that can be used as a first line of investigation. Hence, the application of a simpler and more rapid technique for determining site integrity is preferable. Notably, the development of functional portable optically stimulated luminescence readers, which can generate rapid luminescence measurements in the field, mitigates some of the drawbacks of the advanced luminescence methods (e.g. Sanderson and Murphy, 2010). Over the last decade, the technique has been applied successfully in multiple studies that have characterised stratigraphic sequences of late Quaternary and Holocene age form the Northern Hemisphere (e.g. Muñoz-Salinas et al., 2011; Munyikwa et al., 2012; Kinnaird et al., 2012, 2015, 2017; Gray et al., 2018; Porat et al., 2019; Rother et al., 2019). From the Southern Hemisphere, reported studies include work by Muñoz-Salinas et al. (2014), Portenga and Bishop (2016), and Stone et al. (2015, 2019). Accordingly, this paper presents a case study that employed a portable OSL reader to generate luminescence signals that were used to determine the integrity of a Late Holocene multicomponent archaeological site located within an aeolian dune environment on the Canadian prairies. Through the construction of luminescence profiles (i.e. vertical depictions of the variation of the luminescence signal with depth) using data acquired using the portable OSL reader, the study aims to show that sites that have experienced significant post-depositional disturbances that cannot be discerned visually can be distinguished relatively rapidly from those that have remained intact.

## 2. Study area

The Bodo Archaeological Locality lies within the Bodo Sand Hills region of east-central Alberta in western Canada (Fig. 1). Physiographically, the region is part of the northern Great Plains, and it falls within the subhumid and semiarid Prairie ecozone of central southern Canada (Wolfe et al., 2002). The archaeological locality is situated within the sand dune region just south of a broad east–west trending depression, a relict glacial meltwater channel that now hosts the underfit Eyehill Creek (Fig. 2; Bayrock, 1967a, Bayrock, 1967b).

The Bodo Sand Hills consist of aeolian dunes that reach heights of up to 8 m, most of which are currently stable, although stabilized blowouts on the dunes point to their intermittent reactivation throughout the Holocene. At present, vegetation in the area is mostly fescue grassland (e.g. Munyikwa and Brown, 2014). The location of the dunes and studies of paleowind directions suggest the aeolian deposits were originally derived from the abundant glacigenic sands and silts in the area (Bayrock, 1967a, Bayrock, 1967b; David, 1977; Mulira, 1986; Shetsen, 1990) during the early postglacial period ca. 15,000–14,000 years ago (Munyikwa et al., 2011, Munyikwa et al., 2017). Aeolian deposits of this type are common landforms in the Prairie ecozone of western Canada and, together with buried soil horizons, constitute a valuable palaeoenvironmental proxy record of episodes of landscape instability interspersed with periods of stability, particularly during the mid- to late Holocene (Hopkins and Running, 2000; Wolfe et al., 2001, Wolfe et al., 2002). However, the timing of these oscillations varies between regions, suggesting that localized conditions such as groundwater depths had an effect on dune mobilization (Muhs and Wolfe, 1999). For instance, in southern Alberta, aeolian dune depositional episodes were dated at between 4500 and 230 years which does not exactly coincide with the episodes between 5700 and 140 years ago reported for dunes in south-central Saskatchewan (Wolfe et al., 2001; Wolfe et al., 2002). Although the environment is a major factor in the activation and stabilization of aeolian landforms, cultural activity likely also played a role in shaping these landscapes, both prior to and following the arrival of Euro-Canadians into the region (Wolfe et al., 2007).

The Bodo Archaeological Locality consists of extensive

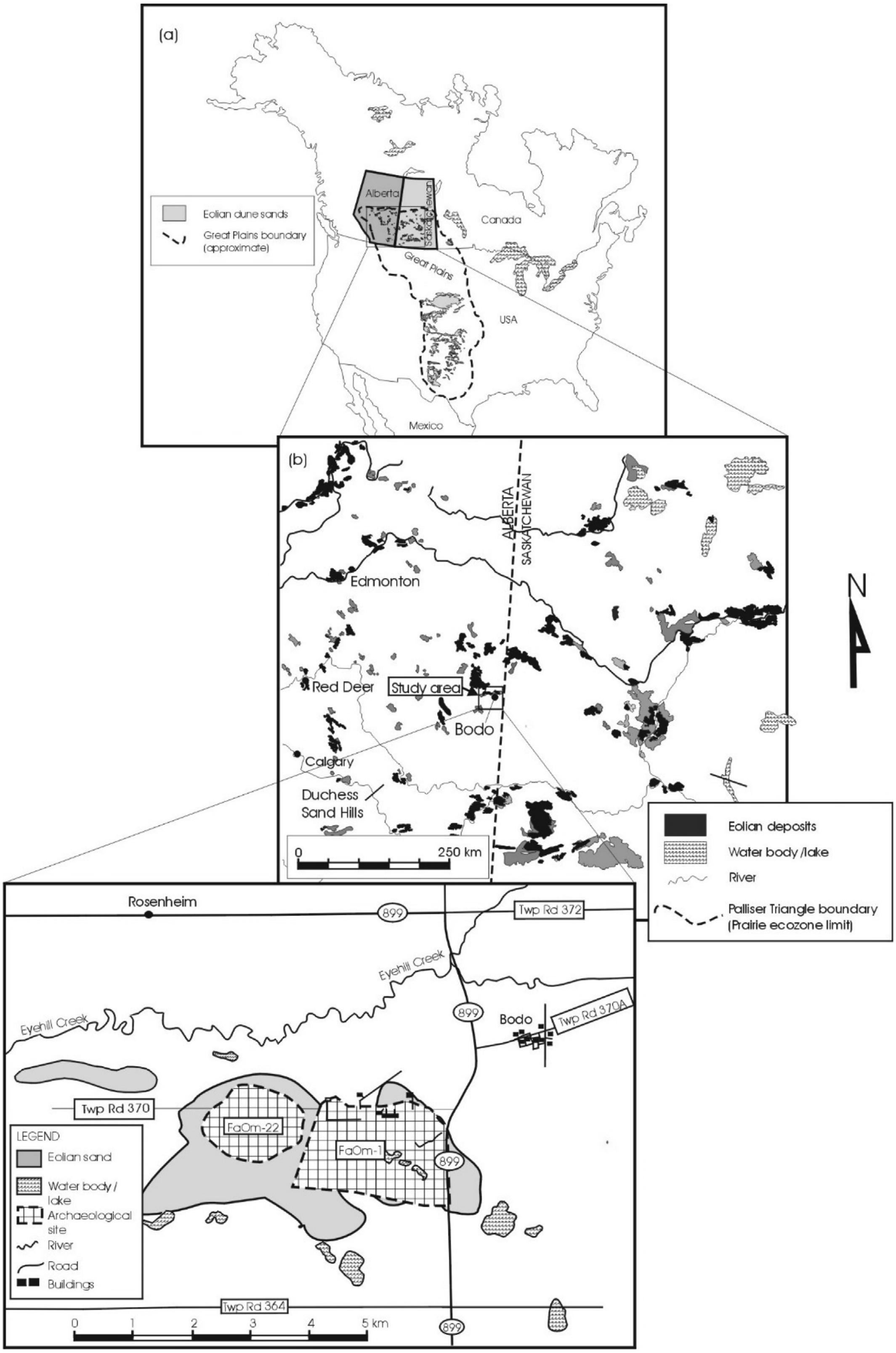


**Fig. 1.** Study area in western Canada: (a) Great Plains of North America with distribution of major aeolian dune deposits (after Muhs and Holliday, 1994, and Wolfe et al., 2000); (b) east-central Alberta, Canada; (c) the Bodo Archaeological Locality showing extent of aeolian deposits (modified after Shetsen, 1990, and Gilliland, 2007).

archaeological deposits spread over an area of at least 800 ha, making it one of the largest Precontact site localities on the northern Great Plains. Consisting of both the Bodo Bison Skulls site (FaOm-1) and the Bodo Overlook site (FaOm-22) (Figs. 1 and 2), the Bodo Archaeological Locality was initially discovered in 1995 during a historic resources impact assessment (HRIA) (Gibson and McKeand, 1996). Subsequent HRIAs and intensive research-based excavations taking place since 2000 have resulted in the recovery of hundreds of thousands of artifacts

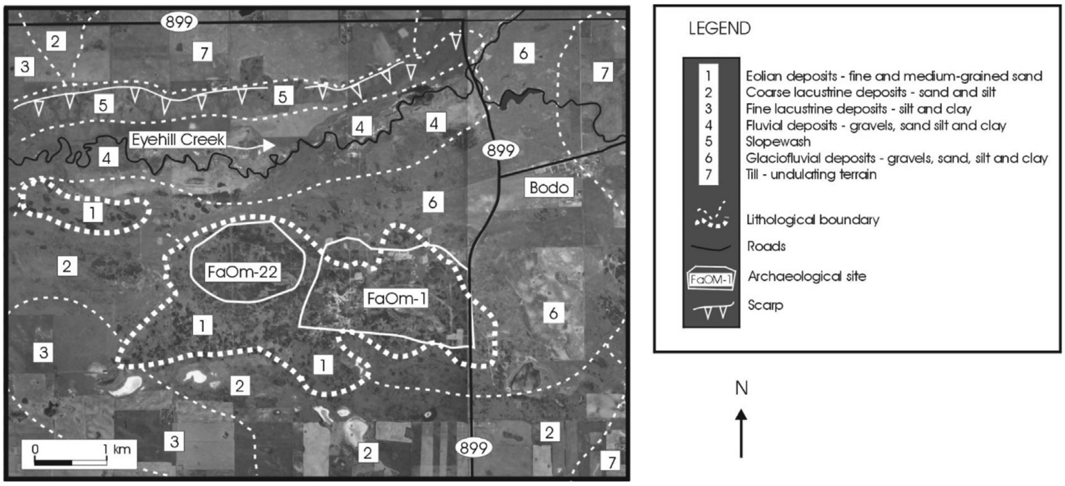


**Fig. 2.** Surficial geology at the Bodo Archaeological Locality. Interpretation based on Bayrock, 1967a, Bayrock, 1967b and Shetsen (1990). Ortho photo flown by Geographic Air Survey, produced by Digital Environmental (Western Heritage Services, Inc.) May 18, 2004.

and demonstrated the extensive nature of the archaeological deposits (Blaikie, 2005; Grekul, 2007; Gibson and Grekul, 2010). Artifactual, stratigraphic, and chronometric evidence indicates the presence of at least three late and middle Precontact-aged occupations (Gilliland, 2007). These correspond to the Old Women's, Mortlach (ca. 1100–250 yr BP) (Vickers, 1986; Dyck and Morlan, 1995), and Sandy Creek phases (ca. 2500–2000 yr BP; Dyck and Morlan, 1995, pp. 389-405; Wettlaufer, 1955) of the Northwestern Plains cultural historical sequence. Surface finds also hint at middle Precontact-aged Oxbow and Duncan occupations (ca. 4600–3000 yr BP; Vickers, 1986), although no *in situ* deposits or chronometric ages have so far been obtained for confirmation.

An HRIA was initiated at FaOm-1 during July 2012 prior to the maintenance of an existing pipeline that was originally installed in the 1970s, before government regulations required historic resources assessments. Common practice during pipeline installation is to minimize landscape disturbance during construction in ecologically sensitive areas by scraping off the topsoil and putting it aside, after which the underlying substrate is worked to the desired level. Following pipeline installation, the pit is back-filled in reverse order, using sediment colour as a guide. Despite these efforts to minimize stratigraphic disruption, sediment mixing is practically unavoidable but may be difficult to detect, especially in settings where colour variations of the depositional units are minor. During the 2012 HRIA, therefore, it was expected that previous pipeline installations had disrupted much of the stratigraphy along the area to be tested, but that pockets of intact deposits could remain. A primary objective of the HRIA was, thus, to identify any intact deposits that could be in conflict with the proposed development and result in unexpected changes in project budget or timelines. To that end, this study aimed to test the applicability of the portable OSL reader in a resource management setting to help identify parts of the tested area that had experienced stratigraphic disruption and distinguish them from intact deposits.

## 3. Methods

### 3.1. HRIA approach, site selection, and sample collection

Given the significance and extent of the archaeological locality, the HRIA focussed on deep testing (up to 70–120 cm below the surface) using 50–100 cm wide pits, excavated by hand. Additionally, the testing had to be directed at areas within 10 metres (m) of either side of the existing pipeline right of way (Gilliland, 2012). For purposes of this case study, three of these pits (BD01, BD02, and BD03A/B; Fig. 3) were sampled for testing using the portable OSL reader. At BD01 and BD02, the excavation and sampling stopped at depths of 90 and 85 cm, respectively. Pit BD03A/B comprises a single pit from which sampling was carried out in two profiles on the north wall, one at either end of the pit, in order to investigate observed stratigraphic differences noted over very short distances, which suggested sediment mixing. In both of these profiles (BD03A and BD03B), sampling was carried out to a depth of 120 cm.

Samples were collected by pushing opaque stainless steel sampling tubes, 2 cm in diameter, at 5 cm intervals into a freshly exposed vertical pit face, after which the open end of the tube was immediately capped. Samples were also collected at the luminescence sampling levels for grain size analysis. The stratigraphy of all three pits was described using standard methods (Day, 1983). Where present, laterally continuous structures such bedding planes or soil horizons were used as indicators of whether the sediments were intact or re-deposited. All pits were back-filled after completing the investigation.

### 3.2. Luminescence analysis

In routine optically stimulated luminescence dating (OSL) studies, luminescence refers to the energy emitted in the form of light by minerals such as quartz and feldspar when stimulated by a light (or heat in thermoluminescence analysis) source (Aitken, 1998). The energy (or dose) accumulates in the mineral grains when radiation damage to lattices of the grains traps electrons. The radiation emanates from naturally occurring isotopes, such as potassium ($^{40}$K), uranium ($^{238}$U and $^{235}$U) and thorium ($^{232}$Th), that are present within the burial environment of the sample. Cosmic radiation also contributes a small but notable fraction (Prescott and Hutton, 1988; Aitken, 1998). Exposure to sunlight releases (zeroes or bleaches) the trapped energy such that mineral grains have to be buried for the dose to accumulate once again. The number of electron traps within any mineral grain is finite and, as long as these traps are not exhausted (saturated), the accumulated signal in a sample grows proportionally with burial age. As a result, the luminescence signal emitted by any sample depends on variables that include the burial age and luminescence sensitivity of the sediment, as well as the local dose rates and level of bleaching experienced prior to burial (Lian and Roberts, 2006, Wintle, 2008). To obtain a luminescence age, two parameters must be determined. The first is the total energy that has accumulated in the sample (called the paleodose) over its burial history. The second is the rate at which the energy has accumulated (i.e. the dose rate). Dividing the paleodose by the dose rate yields the time period that has elapsed since the sample was last zeroed (the burial age). Typically, luminescence measurements for chronometric dating are made in the laboratory using lab-bound luminescence

 

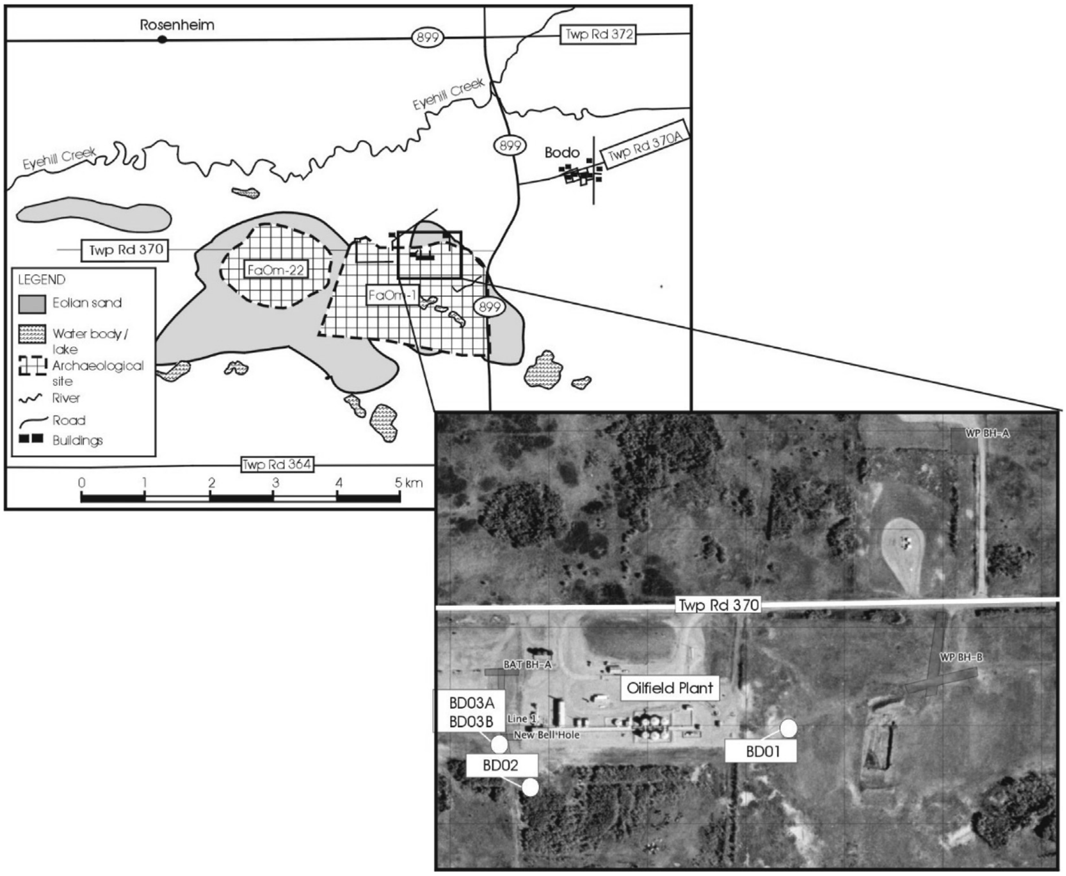


**Fig. 3.** Study area with insert showing location of test pits BD01, BD02 and BD03A/B (BD03A and BD03B), in FaOm-1.

readers (e.g. Bøtter-Jensen, 2000; Bøtter-Jensen et al., 2000), and time-intensive protocols (e.g. Murray and Wintle, 2003).

Apart from producing chronometric ages, however, luminescence measurements can also be used in stratigraphic analysis (e.g. Sanderson and Murphy, 2010). Using this approach, a luminescence profile can be constructed for a given stratigraphic sequence to demonstrate the variation of the luminescence signal with depth. Assuming that the luminescence sensitivities of the mineral grains, the mineralogy, water content, and the environmental dose rates are relatively constant throughout the depositional sequence, the only variable that would determine changes in the signal intensity with depth would be the depositional (or burial) age of the sediments. Thus, in such instances the luminescence profiles can be considered as proxies for the chronostratigraphy, and variations in the accumulated signals with depth can also be seen as reflecting the relative ages of the different units within a depositional sequence (Sanderson and Murphy, 2010).

Measurements for luminescence profiles do not necessarily have to be made using the traditional lab-bound luminescence readers. Portable luminescence readers are employed to rapidly generate signals that can be used to construct luminescence profiles in a fraction of the time it would take using traditional luminescence readers, and with minimal financial input beyond the initial investment in the portable OSL reader (Sanderson and Murphy, 2010). Over the last decade, multiple studies have applied portable luminescence readers to characterise depositional sequences in geomorphological as well as in archaeological investigations by profiling. Geomorphological applications include studies on fluvial sequences (e.g. Muñoz-Salinas et al., 2011, 2014; Portenga et al., 2016), on coastal sequences (e.g. Bateman et al., 2015, 2018; Kinnaird et al., 2012, 2015; Preston et al., 2019), and on inland aeolian depositional systems (e.g. Munyikwa et al., 2012; Stone et al., 2015, 2019; Rother et al., 2019). In archaeological applications, portable OSL reader systems have been used to render insight into depositional sequences at old mine workings (e.g. Mills et al., 2014), on former agricultural terraces (e.g. Kinnaird et al., 2017; Porat et al., 2019) and to elucidate the history of archaeological bridge construction (e.g. Ghilardi et al., 2015). In all instances, profiling using portable OSL readers has been employed to differentiate depositional units on the basis of their luminescence properties, which in most cases are related to the transport or depositional history of the sequences. In settings where luminescence properties have been used to distinguish boundaries between units of different age, gaps in the depositional record or unconformities have been identified (Sanderson and Murphy, 2010; Muñoz-Salinas et al., 2011, 2014; Portenga et al., 2016). Alternatively, where differences in sediment luminescence sensitivity are the sources of contrasts in signal intensity between units, variations in sediment transport and depositional history have been ascertained (e.g. Munoz-Salinas et al., 2014; Portenga et al., 2016; Castillo et al., 2017; Gray et al., 2019). This allows sediment transport, deposition and, possibly, provenance to be elucidated. Profiling also enables screening for purposes of selecting samples that would be appropriate for dating using full-fledged luminescence dating methods. In that way, appropriate depositional units would be targeted for sampling in the field. In other applications, portable OSL readers have been used to approximate sediment ages by calibrating the signals obtained in order to derive paleodoses (e.g. Munyikwa et al., 2014, Stone et al., 2015, 2019; Grey et al., 2018). In this study, however, luminescence profiling is employed to provide sediment characteristics down the depositional sequence in order to identify any variations that may exist. The portable OSL reader used to generate luminescence signals is the instrument developed by the Scottish Universities Environmental Research Centre (SUERC).

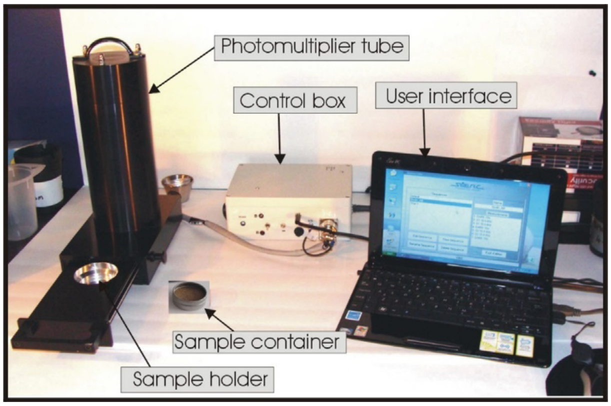


**Fig. 4.** Basic components of a portable OSL reader system.

### 3.3. Portable OSL readers

#### 3.3.1. Basic design

A majority of investigations that have employed portable OSL readers to date have used the SUERC portable OSL reader. The basic components of the second-generation design of the SUERC reader, which was used in this study, include a detector head containing a photomultiplier tube that is mounted over a sample drawer system (Fig. 4). Housed in a separate box is the control unit, which has the switchgear for operation. Power for the system can be derived from the mains grid or, alternatively, from batteries housed in the control box. A laptop computer provides a user interface and data logging capabilities. Samples are introduced into the unit through the drawer in appropriate containers (Sanderson and Murphy, 2010). The SUERC portable OSL reader is capable of both continuous wave (CW mode) as well as pulsed stimulation. The stimulation source outfit contains both an infrared source (IRSL) centred around 880 nm (intended for feldspars) and a blue OSL source centred around 470 nm (intended for quartz). The stimulation collar comprises 6 clustered diode ports in conjunction with RG780 long pass filters for the IR diodes and GG420 long pass filters for the blue diodes. Signal detection occurs through UG11 filters. In synchronous pulsed mode counting, the unit can detect signals below the dark count rate of the instrument (Sanderson and Murphy, 2010).

#### 3.3.2. Operational mode

Since the portable OSL reader can be used on bulk sediment, which usually contains both feldspars and quartz, it is necessary to maximize the signal yielded by the mineral species targeted for stimulation. IRSL stimulation of feldspars in bulk samples is not usually problematic because the fast luminescence component of quartz does not appear to be significantly affected by IR stimulation at temperatures below around 125 °C (e.g. Jain and Singhvi, 2001; Thompsen et al., 2008). Blue light stimulation, however, also causes luminescence in feldspar such that if a bulk sample were to be subjected to blue OSL stimulation, the resultant signal would comprise luminescence from both feldspars and quartz. Notably, a large proportion of the blue-sensitive traps in feldspar are also emptied by extended exposure to IR stimulation (e.g. Jain and Singhvi, 2001). Thus, when the blue-OSL stimulation of a bulk sample containing feldspars and quartz is carried out after first exposing the sample to an IR source, a quartz-dominant signal is obtained, and is referred to as post-IR blue-OSL signal (e.g. Bannerjee et al., 2001; Roberts and Wintle, 2001; Wallinga, Murray and Bøtter-Jensen, 2002); this signal will have a feldspar contribution, albeit a reduced one (e.g. Thompsen et al., 2008). In luminescence profiling, however, it is the relative intensities of luminescence signals with depth that are being examined. Hence, the contamination of a quartz signal by feldspar is not likely to be a problem, unless the feldspar versus quartz abundances vary dramatically up the depositional sequence.

When operating the portable OSL reader in CW mode, the system can be configured to make measurements of the dark-count as well as signal counts following IRSL or post-IR blue-OSL stimulation. These can be presented as integrated signal intensities of either IRSL or post-IR blue-OSL stimulation. In turn, the ratio of the IRSL signal to that of the post-IR blue-OSL signal can be derived and this functions as a proxy for the proportion of feldspar to quartz (Sanderson and Murphy, 2010).

#### 3.3.3. Measurements performed

Four sample portions were measured for each sampled level, and each portion was introduced to the portable OSL reader in a Petri dish measuring 5 cm wide and 1 cm deep with the sediment (about 10 g) completely covering the base of the Petri dish. For each portion run, the measurement protocol employed a 15 seconds (s) dark count, followed by a 60 s IRSL stimulation, after which another 15 s dark count was performed. This was immediately followed by a 60 s blue OSL stimulation (post-IR) and a final 15 s dark count measurement.

When constructing luminescence profiles, it is important to, whenever possible, assess the dose rates at the sampled levels in order to ascertain whether the observed changes in the luminescence profile are an artifact of variations in the dose rates. Hence, in all four stratigraphic profiles (BD01, BD02, BD03A, and BD03B) the concentrations of K, U and Th were measured at the sampled depth using a portable RS-230 Super-spec gamma ray spectrometer. Four separate measurements ($4 \times 120$ s) were carried out for each sample and the concentrations listed in Tables 1–4 are mean values. Overall, the values have errors of around 10–15% and these originate from statistical, calibration and sample geometry errors. Interstitial water in sediment pores attenuates dose received by sediment grains (Aitken, 1998). However, in this study we have not taken variations in water content down the sequence into account for two main reasons. First, the annual rainfall in this part of Alberta is about 250 mm per year. Snowfall contributes approximately an equal amount such that the annual precipitation for the area is around 500 mm per year, and the area is classified as semiarid. Additionally, the near-surface geology of area comprises well-drained sands. As a result, the water table is relatively low throughout the year. Moisture content measurements at comparable depths ($<$ 1.5 m) in the area have previously been shown to be about 5% (e.g. Munyikwa et al., 2014) and, given the low clay content ($<$ 5%), we think differences in moisture content between the upper and lower parts of the sampled pits has been less than 1% during most of the burial history of the sediments. Second, even if we were to assume significant variations in the water content down the stratigraphy, attenuation of dose rates would have increased downwards with increasing moisture content. Notably, however, intact sequences that we measured in this study showed increasing signal intensities with depth before any corrections for moisture content. Hence, this confirms that correcting for moisture content would not have altered our conclusions.

Samples were also analysed for grain size distribution using standard dry sieving methods (e.g. McKeague, 1981). Statistical analyses of the dry sieve measurement results were performed using the GRADISTAT program (Blott and Pye 2001, 2006) and granulometric parameters were determined using the Folk and Ward (1957) method in micron units.

## 4. Results

### 4.1. Section BD01

#### 4.1.1. Stratigraphy

Profile BD01, excavated to 90 cm depth (Fig. 5), consists predominantly of well-sorted aeolian sand to silty sand, with mean grain sizes in the fine to medium size range (Fig. 5, Table 1). Moving upwards from the base of the profile, darker-coloured, thin, organic-rich layers with a silt content of 12–15% are observed at 75–73 cm and 70–67 cm; these are accompanied by evidence of bioturbation by soil fauna and

**Table 1**
Granulometric, luminescence and dosimetric data from Profile BD01.

| Depth (cm) | Sample number | Mean Grain Size (μm) | Sorting* | IRSL (photon counts × 1000) | Post- IR Blue OSL (photon counts × 1000) | IRSL/Post–IR Blue OSL‡ | K § (%) | U (ppm) | Th (ppm) |
|---|---|---|---|---|---|---|---|---|---|
| 5 | BD01-1 | 243 | w.s. | 0.8 ± 0.06 | 5.0 ± 0.1 | 0.16 | 1.2 | 1.2 | 3.0 |
| 10 | BD01-2 | 254 | w.s. | 8.0 ± 0.1 | 18.1 ± 0.2 | 0.44 | 1.4 | 1.7 | 2.9 |
| 15 | BD01-3 | 250 | w.s. | 18.3 ± 0.2 | 47.5 ± 0.2 | 0.39 | 1.4 | 1.7 | 2.9 |
| 20 | BD01-4 | 239 | w.s. | 30.5 ± 0.2 | 59.9 ± 0.3 | 0.51 | 1.4 | 1.6 | 3.0 |
| 25 | BD01-5 | 248 | w.s. | 36.5 ± 0.2 | 73.5 ± 0.3 | 0.50 | 1.6 | 1.1 | 3.9 |
| 30 | BD01-6 | 247 | w.s. | 34.0 ± 0.2 | 69.6 ± 0.3 | 0.50 | 1.6 | 1.6 | 3.3 |
| 35 | BD01-7 | 237 | m.w.s. | 32.6 ± 0.2 | 74.8 ± 0.3 | 0.43 | 1.6 | 1.7 | 4.0 |
| 40 | BD01-8 | 248 | w.s. | 37.7 ± 0.3 | 79.2 ± 0.3 | 0.48 | 1.8 | 1.5 | 3.8 |
| 45 | BD01-9 | 265 | w.s. | 39.0 ± 0.2 | 77.7 ± 0.3 | 0.50 | 1.7 | 1.4 | 3.0 |
| 50 | BD01-10 | 269 | w.s. | 39.4 ± 0.2 | 75.9 ± 0.3 | 0.52 | 1.6 | 1.5 | 4.8 |
| 55 | BD01-11 | 262 | w.s. | 42.5 ± 0.2 | 82.3 ± 0.3 | 0.52 | 1.6 | 1.7 | 2.9 |
| 60 | BD01-12 | 261 | w.s. | 41.0 ± 0.2 | 74.7 ± 0.3 | 0.55 | 2.6 | 1.7 | 3.5 |
| 65 | BD01-13 | 256 | w.s. | 49.6 ± 0.2 | 83.0 ± 0.3 | 0.60 | 1.7 | 1.8 | 3.9 |
| 70 | BD01-14 | 248 | w.s. | 51.5 ± 0.2 | 97.4 ± 0.3 | 0.53 | 1.8 | 1.8 | 3.7 |
| 75 | BD01-15 | 258 | w.s. | 51.6 ± 0.2 | 94.5 ± 0.3 | 0.55 | 1.8 | 1.8 | 3.8 |
| 80 | BD01-16 | 264 | w.s. | 47.3 ± 0.2 | 98.2 ± 0.3 | 0.48 | 1.8 | 1.8 | 4.1 |
| 85 | BD01-17 | 266 | w.s. | 62.7 ± 0.3 | 124.0 ± 0.4 | 0.51 | 1.8 | 1.8 | 4.6 |
| 90 | BD01-18 | 265 | w.s. | 225.3 ± 0.5 | 453.2 ± 0.8 | 0.50 | 1.8 | 1.8 | 3.4 |

*Abbrev. w.s. – well sorted m.w.s. moderately well sorted. ‡The IRSL/Post-IR blue OSL ratio is a proxy of the feldspar to quartz ratio.
§ K, U and Th are responsible for the irradiation that gives rise to the luminescence energy stored in the sediment grains.

the presence of rare roots, indicating pedogenesis. From the depth of about 65 cm, the silt content decreases slightly to less than 10% and iron mottling can be observed in the brown sands up to the depth of 40 cm. Between 40 and 30 cm, slightly darker colours than the surrounding sediment are also observed and the silt content increases to about 10–12%. Above this level (30–20 cm), the silt content of the sands decreases to less than 5% to give brown medium to fine-grained aeolian sand (Fig. 5a,b). From around 20–12 cm, the sediment grades into dark grayish brown silty sand but at around 12–10 cm, the sediment transitions to very dark brown silty sand with a silt content of around 12–15%. The upper ~8–10 cm of the section comprises dark grayish brown silty sand on which the contemporary soil is developing. Artifacts are present from 20 cm depth to the surface, and consist primarily of bone fragments and a lithic flake.

#### 4.1.2. Portable OSL reader luminescence profiles

The luminescence profiles for Profile BD01 generally show signal intensities that decrease consistently up the depositional sequence (Fig. 5c, d, Table 1). From the base of the section, the IRSL signal intensity decreases sharply, falling to less than 28% of the value seen at 90–85 cm near the surface. From 80 to 25 cm, however, the drop in the signal intensity is more gradual, falling from around 50,000 to around 36,000 counts. In the upper part of the section (35–5 cm), the signal intensity decreases from 36,000 to around 8000 counts. The post-IR blue OSL signal profile essentially mirrors that of the IRSL signal.

The IRSL/OSL ratio, which can be seen as an approximate measure of the proportion of feldspar to quartz, is relatively stabilized at around 0.5 between depths of 90–20 cm, with minor fluctuations suggesting slight variations in mineral abundances up the profile (Fig. 5e). From 15 to 5 cm, however, the IRSL/OSL ratio drops from 0.39 to 0.16, possibly as a result of a decrease in the proportion of feldspar in the sediment, likely due to increased weathering during soil formation close to the modern surface.

### 4.2. Section BD02

#### 4.2.1. Stratigraphy

Excavated to 85 cm depth (Fig. 6), the profile at BD02 comprises predominantly well-sorted fine- to medium-sized aeolian sands and silty sands. From 80 to 50 cm are brown sands with a silt content of less than 5%. Further upwards, from around 50–40 cm, the silt content increases to more than 15% and the colour of the sands changes to

**Table 2**
Granulometric, luminescence and dosimetric data from Profile BD02.

| Depth | Sample Number | Mean Grain Size (μm) | Sorting* | IRSL (photon counts × 1000) | Post- IR Blue OSL (photoncounts × 1000) | IRSL/Post–IR Blue OSL‡ | K§ (%) | U (ppm) | Th (ppm) |
|---|---|---|---|---|---|---|---|---|---|
| 5 | BD02-1 | 241 | w.s. | 2.8 ± 0.1 | 10.6 ± 0.1 | 0.26 | 1.3 | 1.6 | 3.4 |
| 10 | BD02-2 | 239 | w.s. | 5.5 ± 0.1 | 13.8 ± 0.1 | 0.39 | 1.4 | 1.6 | 2.6 |
| 15 | BD02-3 | 247 | w.s. | 5.2 ± 0.1 | 14.8 ± 0.1 | 0.35 | 1.4 | 1.4 | 3.0 |
| 20 | BD02-4 | 250 | w.s. | 5.6 ± 0.1 | 16.7 ± 0.1 | 0.33 | 1.5 | 1.5 | 1.3 |
| 25 | BD02-5 | 250 | w.s. | 6.1 ± 0.1 | 16.7 ± 0.2 | 0.37 | 1.3 | 1.4 | 2.8 |
| 30 | BD02-6 | 246 | w.s. | 6.7 ± 0.1 | 16.3 ± 0.2 | 0.40 | 1.6 | 1.6 | 3.4 |
| 35 | BD02-7 | 242 | w.s. | 10.4 ± 0.1 | 18.8 ± 0.2 | 0.55 | 1.6 | 1.2 | 2.9 |
| 40 | BD02-8 | 234 | w.s. | 9.1 ± 0.1 | 16.9 ± 0.2 | 0.54 | 1.9 | 1.8 | 4.0 |
| 45 | BD02-9 | 240 | w.s. | 11.3 ± 0.1 | 20.2 ± 0.2 | 0.56 | 1.6 | 1.5 | 2.4 |
| 50 | BD02-10 | 243 | w.s. | 22.9 ± 0.1 | 45.8 ± 0.2 | 0.50 | 1.8 | 1.4 | 2.9 |
| 55 | BD02-11 | 243 | w.s. | 28.2 ± 0.2 | 57.9 ± 0.3 | 0.49 | 1.9 | 1.3 | 4.4 |
| 60 | BD02-12 | 235 | w.s. | 27.9 ± 0.2 | 55.8 ± 0.3 | 0.49 | 1.8 | 2.3 | 2.5 |
| 65 | BD02-13 | 236 | w.s. | 37.4 ± 0.2 | 78.9 ± 0.3 | 0.47 | 1.7 | 1.9 | 2.9 |
| 70 | BD02-14 | 235 | w.s. | 35.5 ± 0.2 | 78.9 ± 0.3 | 0.45 | 1.9 | 2.1 | 3.5 |
| 75 | BD02-15 | 242 | w.s. | 35.3 ± 0.2 | 75.9 ± 0.3 | 0.47 | 1.8 | 1.6 | 3.6 |
| 80 | BD02-16 | 238 | w.s. | 37.3 ± 0.2 | 80.2 ± 0.3 | 0.47 | 1.8 | 1.9 | 3.9 |

*Abbrev. w.s. – well sorted ‡The IRSL/Post-IR blue OSL ratio is a proxy of the feldspar to quartz ratio.
§ K, U and Th are responsible for the irradiation that gives rise to the luminescence energy stored in the sediment grains.

**Table 3**
Granulometric, luminescence and dosimetric data from Profile BD03A.

| Depth | Sample Number | Mean Grain Size (μm) | Sorting* | IRSL (photon counts × 1000) | Post- IR Blue OSL (photon counts × 1000) | IRSL/Post-IR Blue OSL‡ | K§ (%) | U (ppm) | Th (ppm) |
|---|---|---|---|---|---|---|---|---|---|
| 5 | BD03A-1 | 250 | w.s. | 44.6 ± 0.3 | 96.6 ± 0.3 | 0.46 | 1.2 | 1.2 | 2.8 |
| 10 | BD03A-2 | 253 | w.s. | 24.0 ± 0.3 | 53.3 ± 0.3 | 0.45 | 1.5 | 1.5 | 2.9 |
| 15 | BD03A-3 | 253 | w.s. | 12.2 ± 0.2 | 59.3 ± 0.3 | 0.24 | 1.4 | 1.8 | 2.9 |
| 20 | BD03A-4 | 246 | w.s. | 11.0 ± 0.1 | 28.8 ± 0.2 | 0.38 | 1.6 | 1.1 | 3.9 |
| 25 | BD03A-5 | 255 | w.s. | 8.7 ± 0.1 | 22.2 ± 0.2 | 0.39 | 1.4 | 1.5 | 4.1 |
| 30 | BD03A-6 | 254 | w.s. | 7.3 ± 0.2 | 25.0 ± 0.2 | 0.29 | 1.7 | 0.9 | 4.2 |
| 35 | BD03A-7 | 252 | w.s. | 22.0 ± 0.2 | 50.8 ± 0.2 | 0.43 | 1.6 | 1.5 | 4.3 |
| 40 | BD03A-8 | 261 | w.s. | 48.5 ± 0.2 | 10.9 ± 0.3 | 4.40 | 1.8 | 1.2 | 4.2 |
| 45 | BD03A-9 | 264 | w.s. | 43.3 ± 0.2 | 94.6 ± 0.3 | 0.45 | 1.6 | 1.5 | 3.3 |
| 50 | BD03A-10 | 261 | w.s. | 38.2 ± 0.2 | 87.5 ± 0.3 | 0.43 | 1.7 | 2.2 | 3.6 |
| 55 | BD03A-11 | 257 | w.s. | 46.6 ± 0.2 | 105.5 ± 0.3 | 0.44 | 1.7 | 1.9 | 3.5 |
| 60 | BD03A-12 | 253 | w.s. | 38.0 ± 0.2 | 83.1 ± 0.3 | 0.46 | 1.7 | 1.6 | 3.0 |
| 65 | BD03A-13 | 260 | w.s. | 47.6 ± 0.2 | 92.6 ± 0.3 | 0.51 | 1.7 | 1.5 | 4.9 |
| 70 | BD03A-14 | 260 | w.s. | 47.6 ± 0.2 | 95.0 ± 0.3 | 0.49 | 1.7 | 1.5 | 5.2 |
| 75 | BD03A-15 | 274 | w.s. | 44.5 ± 0.2 | 91.7 ± 0.3 | 0.49 | 1.8 | 1.6 | 3.1 |
| 80 | BD03A-16 | 280 | w.s. | 47.5 ± 0.2 | 87.9 ± 0.3 | 0.54 | 1.7 | 1.6 | 4.2 |
| 85 | BD03A-17 | 260 | w.s. | 44.4 ± 0.2 | 87.8 ± 0.3 | 0.51 | 1.8 | 1.5 | 4.5 |
| 90 | BD03A-18 | 267 | w.s. | 38.0 ± 0.2 | 81.3 ± 0.3 | 0.47 | 1.8 | 2.3 | 4.8 |
| 95 | BD03A-19 | 270 | w.s. | 37.8 ± 0.2 | 81.9 ± 0.3 | 0.46 | 1.8 | 1.8 | 4.9 |
| 100 | BD03A-20 | 279 | w.s. | 39.8 ± 0.2 | 81.0 ± 0.3 | 0.49 | 1.8 | 1.5 | 5.0 |
| 105 | BD03A-21 | 268 | w.s. | 43.8 ± 0.2 | 95.2 ± 0.3 | 0.46 | 1.8 | 1.7 | 5.2 |
| 110 | BD03A-22 | 265 | w.s. | 46.0 ± 0.2 | 87.0 ± 0.3 | 0.53 | 1.9 | 2.2 | 4.1 |
| 115 | BD03A-23 | 262 | w.s. | 36.7 ± 0.2 | 71.2 ± 0.3 | 0.51 | 1.7 | 1.3 | 4.7 |
| 120 | BD03A-24 | 260 | w.s. | 36.9 ± 0.2 | 69.4 ± 0.2 | 0.53 | 1.8 | 2.3 | 4.9 |

*Abbrev. w.s. – well sorted ‡The IRSL/Post-IR blue OSL ratio is a proxy of the feldspar to quartz ratio.
§ K, U and Th are responsible for the irradiation that gives rise to the luminescence energy stored in the sediment grains.

black. Bone fragments can be identified in this horizon and we interpret it to represent a buried former soil surface. Between 40 cm and around 30 cm, the silt content drops to less than 10% and the colour of the sands grades to dark grayish brown. From 30 to 23 cm, the sands transition to black once again and the silt content rises to more than 10%. We interpret this to be another intact buried soil. Artifacts associated with the soil include bone fragments, lithic flakes, and one complete Late Side-notched projectile point that is typologically consistent with the Late Precontact-aged Old Women's phase in the Northwestern Plains cultural historical sequence (1100–250 yr BP; Peck, 2011; Vickers, 1986; Fig. 7). This buried soil is overlain by dark brown sands that extend from 23 to 12 cm. The upper around 12 cm of the sequence comprise black silty sands that represent soil forming processes acting on the modern surface.

#### 4.2.2. Luminescence profiles

The IRSL and post-IR OSL signal plots from Profile BD02 are relatively similar to those from Profile BD01, in that high signal intensities

**Table 4**
Granulometric, luminescence and dosimetric data from Profile BD03B.

| Depth | Sample Number | Mean Grain Size (μm) | Sorting* | IRSL (photon counts × 1000) | Post- IR Blue OSL (photon counts × 1000) | IRSL/Post–IR Blue OSL ‡ | K§ (%) | U (ppm) | Th (ppm) |
|---|---|---|---|---|---|---|---|---|---|
| 5 | BD03B-1 | 252 | w.s. | 48.9 ± 0.3 | 79.8 ± 0.3 | 0.61 | 1.2 | 0.9 | 3.4 |
| 10 | BD03B-2 | 248 | w.s. | 8.9 ± 0.2 | 30.1 ± 0.2 | 0.49 | 1.4 | 0.9 | 3.1 |
| 15 | BD03B-3 | 251 | w.s. | 9.0 ± 0.2 | 24.6 ± 0.2 | 0.40 | 1.4 | 1.4 | 2.9 |
| 20 | BD03B-4 | 254 | w.s. | 6.7 ± 0.2 | 20.7 ± 0.2 | 0.30 | 1.4 | 1.3 | 3.3 |
| 25 | BD03B-5 | 252 | w.s. | 7.9 ± 0.2 | 21.7 ± 0.2 | 0.32 | 1.3 | 1.4 | 3.1 |
| 30 | BD03B-6 | 252 | w.s. | 2.8 ± 0.2 | 12.9 ± 0.1 | 0.21 | 1.6 | 1.4 | 4.0 |
| 35 | BD03B-7 | 250 | w.s. | 9.5 ± 0.2 | 24.4 ± 0.2 | 0.40 | 1.6 | 1.7 | 2.8 |
| 40 | BD03B-8 | 252 | w.s. | 8.9 ± 0.2 | 22.8 ± 0.2 | 0.40 | 1.5 | 1.6 | 3.8 |
| 45 | BD03B-9 | 256 | w.s. | 9.0 ± 0.2 | 25.3 ± 0.2 | 0.36 | 1.6 | 1.9 | 3.6 |
| 50 | BD03B-10 | 255 | w.s. | 6.7 ± 0.2 | 19.4 ± 0.2 | 0.35 | 1.7 | 1.1 | 4.2 |
| 55 | BD03B-11 | 262 | w.s. | 7.9 ± 0.2 | 25.5 ± 0.2 | 0.31 | 1.7 | 2.2 | 3.1 |
| 60 | BD03B-12 | 264 | w.s. | 9.2 ± 0.1 | 26.7 ± 0.2 | 0.34 | 1.6 | 1.6 | 4.1 |
| 65 | BD03B-13 | 260 | w.s. | 13.9 ± 0.1 | 32.6 ± 0.2 | 0.42 | 1.8 | 1.4 | 4.2 |
| 70 | BD03B-14 | 259 | w.s. | 14.6 ± 0.1 | 31.0 ± 0.2 | 0.47 | 1.8 | 1.5 | 4.9 |
| 75 | BD03B-15 | 255 | w.s. | 20.0 ± 0.1 | 43.2 ± 0.2 | 0.46 | 1.7 | 2.1 | 4.4 |
| 80 | BD03B-16 | 262 | w.s. | 24.4 ± 0.1 | 52.0 ± 0.3 | 0.47 | 2.0 | 1.3 | 4.8 |
| 85 | BD03B-17 | 264 | w.s. | 28.3 ± 2.0 | 59.7 ± 0.3 | 0.53 | 1.8 | 1.4 | 4.8 |
| 90 | BD03B-18 | 265 | w.s. | 34.5 ± 0.2 | 64.4 ± 0.3 | 0.42 | 1.8 | 1.6 | 4.8 |
| 95 | BD03B-19 | 259 | w.s. | 26.2 ± 0.2 | 55.0 ± 0.3 | 0.48 | 2.1 | 2.1 | 4.0 |
| 100 | BD03B-20 | 264 | w.s. | 36.1 ± 0.2 | 75.3 ± 0.3 | 0.48 | 1.7 | 1.6 | 4.5 |
| 105 | BD03B-21 | 256 | w.s. | 37.3 ± 0.02 | 74.5 ± 0.3 | 0.50 | 2.0 | 1.8 | 4.1 |
| 110 | BD03B-22 | 259 | w.s. | 30.6 ± 0.2 | 54.8 ± 0.3 | 0.56 | 1.9 | 2.4 | 4.7 |
| 115 | BD03B-23 | 260 | w.s. | 34.5 ± 0.2 | 62.9 ± 0.3 | 0.55 | 1.8 | 2.8 | 5.3 |
| 120 | BD03B-24 | 261 | w.s. | 42.5 ± 0.2 | 80.3 ± 0.3 | 0.53 | 1.9 | 2.4 | 5.0 |

*Abbrev. w.s. – well sorted ‡The IRSL/Post-IR blue OSL ratio is a proxy of the feldspar to quartz ratio.
§ K, U and Th are responsible for the irradiation that gives rise to the luminescence energy stored in the sediment grains.

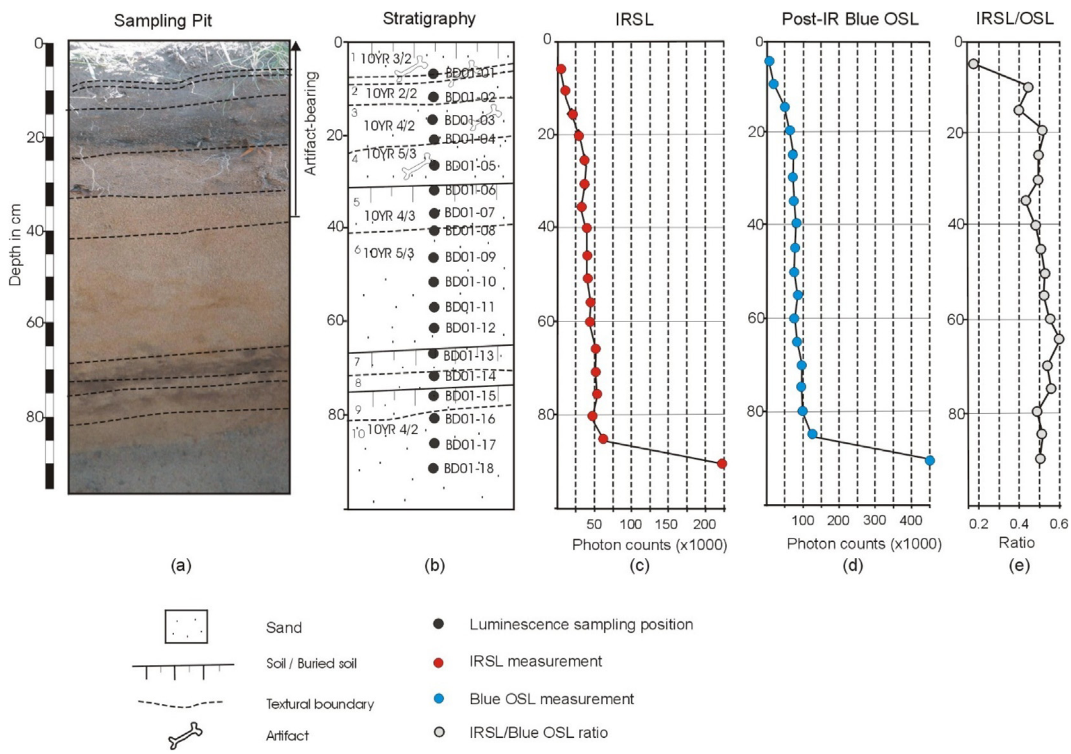


**Fig. 5.** Stratigraphy and luminescence profiles from Profile BD01. (a) Sampling pit excavated at site. (b) The sampling positions as well as Munsell colours of sediments are shown in the stratigraphic section. The IRSL signal (c) is emitted by feldspar grains and the post-IR blue OSL signal (d) is predominantly from quartz. Hence, the IRSL/OSL ratio (e) approximates the relative proportions of feldspar to quartz in the sample portion.

are noted in the lower part of the profile and these decrease up the profile (Fig. 6c, d, Table 2). From 85 to 65 cm from the surface, the IRSL signal intensity is relatively stable at about 37,000 counts. Between 65 and 60 cm, however, there is a sharp drop in the signal intensity to around 28,000 counts. This is followed by a more gradual decline between 60 and 50 cm to around 23,000 counts. From 50 to 45 cm, another relatively rapid decrease is noticed, with the signal falling to 11,000 counts. The signal then remains relatively stable up to 35 cm,

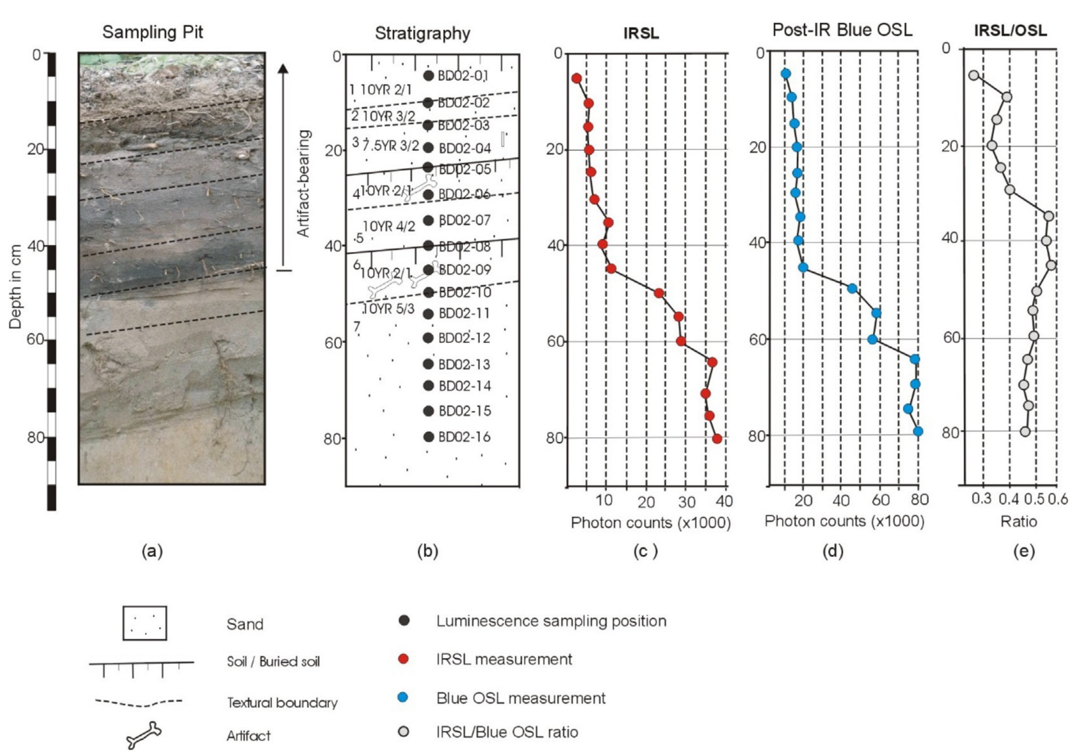


**Fig. 6.** Stratigraphy and luminescence profiles from Profile BD02. (a) Sampling pit excavated at site. (b) The sampling positions and Munsell colours of sediments are shown in the stratigraphic section. The IRSL signal (c) is emitted by feldspar grains and the post-IR blue OSL signal (d) is predominantly from quartz. (e) The IRSL/OSL ratio approximates the relative proportions of feldspar to quartz in the sample.


**Fig. 7.** Late Side-notched projectile point recovered from buried soil, 28–22 cm below the surface, Profile BD02.

after which it gradually falls to about 5000 counts between 30 and 10 cm before it tapers off to around 3000 at the depth of 5 cm from the surface. The post-IR OSL signal profile essentially mirrors that of the IRSL signal, demonstrating a stepwise decrease in signal intensity between 65 and 60, 60–50, 50–45, 35–30, 30–10 and 10–5 cm (Fig. 6d).

From the base of the section to 35 cm, the IRSL/OSL ratio remains relatively stable at about 0.50, fluctuating by less than 10% (Fig. 6e). From 30 cm to surface, the ratio is comparatively lower (0.26–0.40), suggesting a lower feldspar content in the upper part of the profile, possibly as a result of weathering during soil forming processes or through abrasion during sediment transport.

### 4.3. Section BD03A

#### 4.3.1. Stratigraphy

The north wall of Profile BD03 (excavated to 120 cm depth) was sampled on both the western (BD03A) (Fig. 8) and eastern ends (BD03B) (Fig. 9) of the section, as these demonstrated observable differences in stratigraphy over a very short distance, suggesting post-depositional disturbance, especially in the eastern end. The lower part of the west end of the profile (120–47 cm) consists of medium-grained well-sorted brown aeolian sand with a silt content of 5–8%. A sharp contact separates the lower unit from the upper unit, which measures from about 47 cm to surface. The dominant sediment of the upper unit is mottled and mixed-looking black to very dark grayish brown well-sorted medium silty sand with a silt content of 12–15%. This pit is located proximal to a buried pipeline and we strongly suspect that the observed mixed-looking upper unit and the sharp contact between the upper and lower units reflects disturbance from previous pipeline activities. Artifacts are present from 47 to 0 cm, and include bone fragments and lithic flakes.

#### 4.3.2. Luminescence profiles

Unlike in profiles BD01 and BD02 where the signal intensities decrease consistently up the depositional sequence, the signals noted in profile BD03A display a more complex pattern. From the bottom of the profile (120 cm) to around 80 cm from the surface, the IRSL signal intensities fluctuate between 48,000 and 36,000 counts, peaking at 110 and 80 cm (Fig. 8c). Between 80 and 65 cm, the signal remains relatively stable, after which it fluctuates again by about 20% up to 40 cm. There is a sharp decrease in the signal from 48,500 to 22,000 (< 50%) between 40 and 35 cm; this decrease occurs about 10 cm above the well-defined contact between the upper and lower units noted in the stratigraphy (i.e. at about 47 cm below the surface; Fig. 8b). At 30 cm, the signal drops further to around 7000 counts, after which it increases relatively gradually to around 12,000 counts at 15 cm. From 10 to 5 cm below the surface, the signal rises sharply to peak at 45,000 counts.

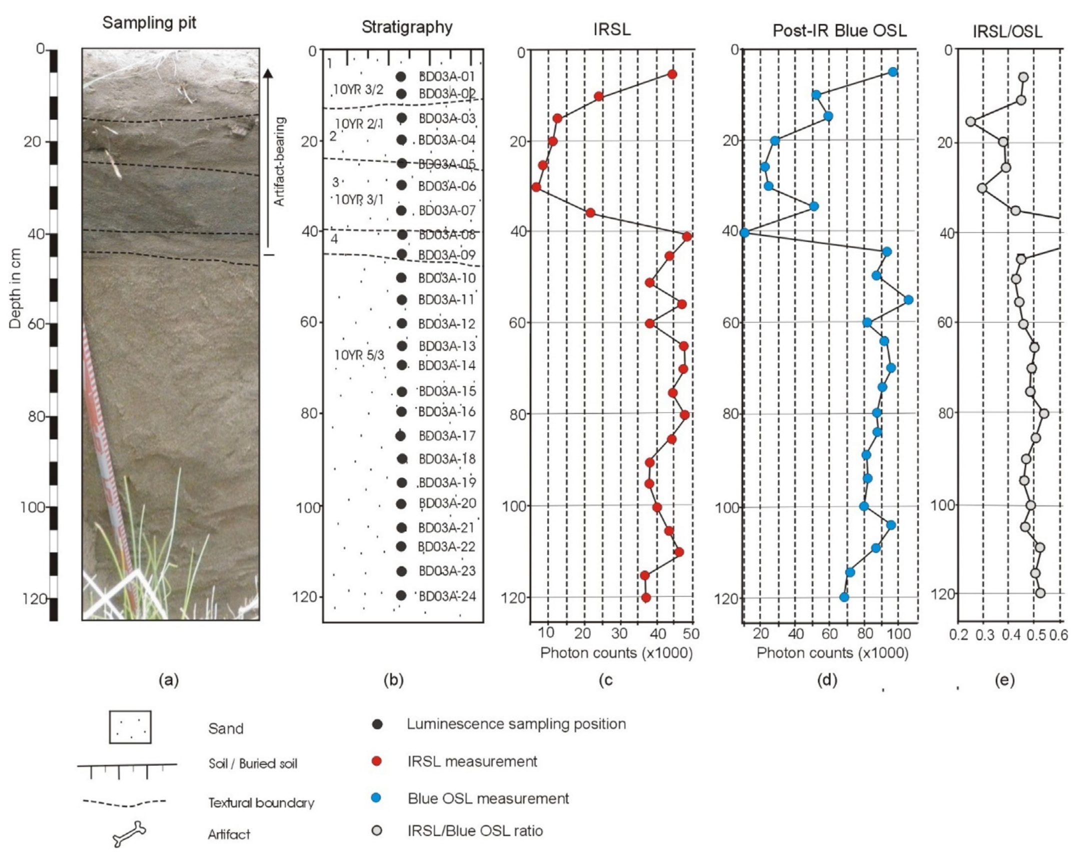


**Fig. 8.** Stratigraphy and luminescence profiles from Profile BD03A. (a) Sampling pit excavated at the site. Note the homogeneous, undisturbed-looking sediments below the artifact-bearing layer. (b) The sampling positions and Munsell colours of the sediments. The IRSL signal (c) is emitted by feldspar grains and the post-IR blue OSL signal (d) is predominantly from quartz. (e) The IRSL/OSL ratio approximates the relative proportions of feldspar to quartz in the sample portion. An anomalously high IRSL/OSL ratio (value 4.4) resulting from a high IRSL signal and a low OSL signal was obtained at depth 40 cm.

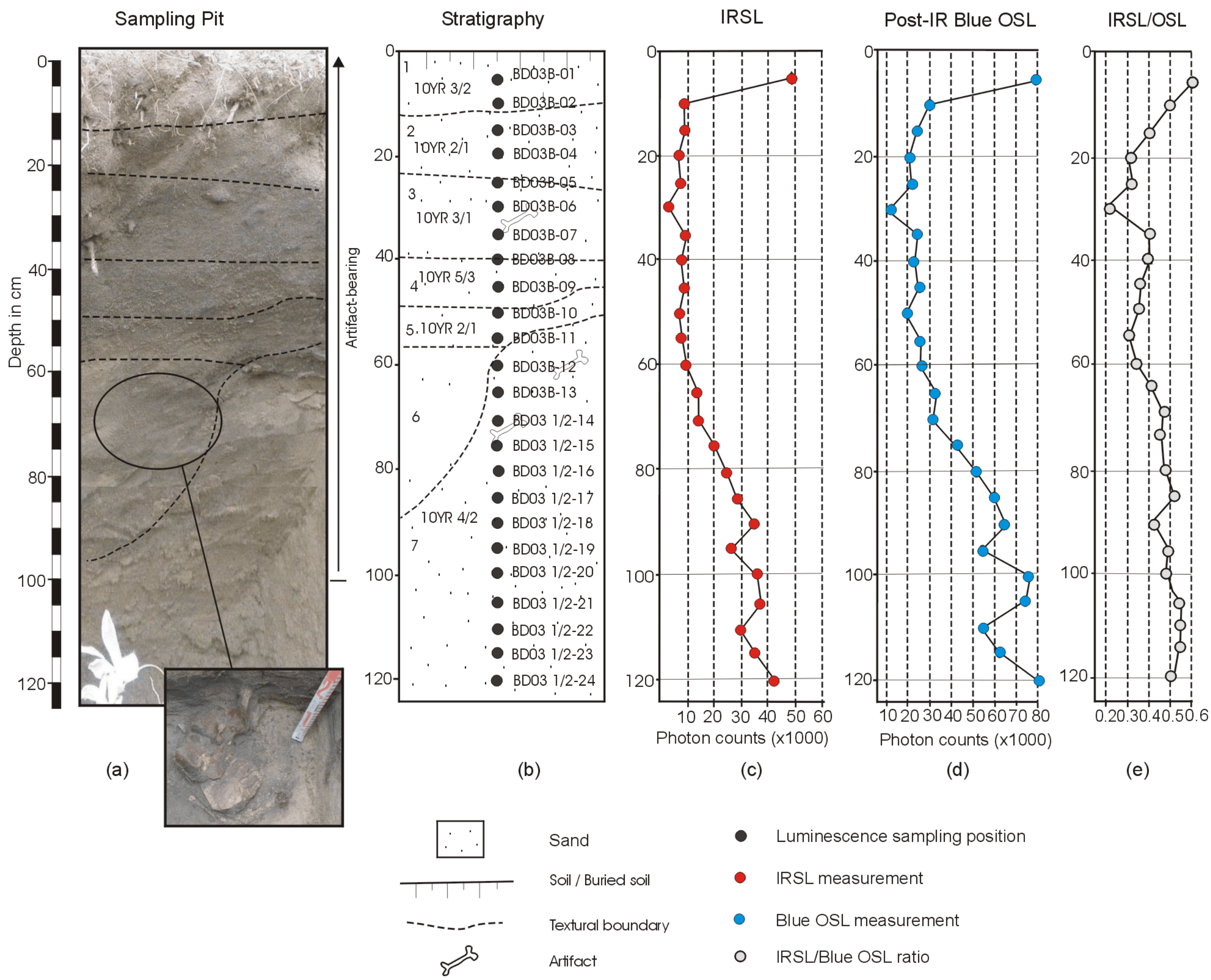

**Fig. 9.** Stratigraphy and luminescence profiles from Profile BD03B. a) Sediments were artifact-bearing to 90 cm depth. Circle delineates darker sediment from which three articulated *Bison bison* vertebrae were recovered (insert). (b) The sampling positions as well as the Munsell colours of the sediments. (c) IRSL signal obtained from feldspar grains. (d) Post-IR blue OSL including quartz signal. (e) The IRSL/OSL ratio approximates the relative proportions of feldspar to quartz in the sample portion.

The shape of the post-IR blue OSL profile (Fig. 8d) demonstrates a trend that is similar to that of the IRSL profile, in that it can be separated into a lower (120–45 cm) and an upper segment (40–5 cm). In the lower segment, signal intensities are up to 700% or more greater than the lowest signal intensity noted in the upper part of the profile, and fluctuate by around 20%. At 40 cm, however, the post –IR OSL signal drops sharply to around 10,000 counts, after which it rises briefly at 35 cm before falling again at 30 cm. From 25 cm upwards, the signal rises to peak just below the surface at about 96,000 counts.

The IRSL/OSL ratio of Profile BD03A is relatively stable from depth to 35 cm, fluctuating between 0.50 and 0.45, with the exception of the ratio at 40 cm where it spikes to a value of around 4 before dropping to the mean value. This could be the result of a very low quartz content in the portion analysed. Alternatively, it could be caused by low luminescence sensitivity of the quartz grains in the sample. Lower magnitude fluctuations in the IRSL/OSL ratio are observed from 30 cm to the surface, with the lower IRSL signals suggesting lower proportions of feldspar especially at depths of 30 and 15 cm.

### 4.4. Section BD03B

#### 4.4.1. Stratigraphy

Section BD03B is the east end of the north wall of the pit excavated at Profile BD03 (Fig. 9). The lower part of the profile (120–100 cm) comprises well-sorted medium-grained brown aeolian sands with a silt content of less than 10%. From 100 to 47 cm, however, a range of colours are noted, including brown, dark grayish black, and black medium-grained well-sorted sands with a silt content of more than 10%. Mottled-looking and bioturbated sediments are present between 60 and 50 cm, and charcoal flecks are noted from 55 to 47 cm. These features and colour variations are not laterally continuous and are not observed on the west end of Profile BD03 (BD03A). Our field interpretations are that these colour variations and stratigraphic disruptions are the result of post-depositional sediment mixing, either as a result of backfilling after pipeline installation or infilling of an animal burrow. The upper part of profile BD03B is relatively similar to that of BD03A on the west end of the section and comprises black to very dark grayish brown well-sorted medium grained silty sand.

An additional difference between the sequences noted on the west end (BD03A) and east end of the section (BD03B) is in the type and distribution of archaeological artifacts recovered. In the east end of the section, artifacts are present throughout the upper 100 cm of the profile whereas, in the west end, they are confined to the upper 47 cm. Artifacts recovered from BD03B include numerous complete skeletal elements from *Bison bison* (P. McKeand, pers. comm.), burnt, unburnt, and calcined bone fragments, pottery sherds, lithic flakes, and charcoal fragments.

#### 4.4.2. Luminescence profile

The IRSL signal profile at BD03B fluctuates between extremes of about 42,000 at the base of the section (120 cm) to about 26,000 around 95 cm, after which there is a gradual decrease up the sequence from 35,000 at 90 cm to 10,000 at 60 cm. From 60 to 10 cm, the signal is relatively constant at between 6000 and 9000 counts, except for the sharp drop at 30 cm (3000 counts; Fig. 9c). Between 10 and 5 cm, the signal trend at BD03B is similar to that observed at the adjacent BD03A in that there is a five-fold increase in the signal intensities from 10,000 to 50,000 counts. The post-IR blue OSL profile is relatively identical to that of the IRSL profile and all fluctuations observed in Fig. 9c are mirrored in Fig. 9d.

The IRSL/OSL ratio is relatively stable around 0.5 between 120 and 70 cm (Fig. 9e), fluctuating by less than 10%. From 65 to 35 cm, however, the signal varies between 0.42 and 0.3, after which it decreases sharply to around 0.2 at 30 cm, followed by an increase to 0.6 at 5 cm.

## 5. Discussion

The core rationale employed in this study is that if clastic sediments are well zeroed of any previously acquired luminescence energy prior to their last burial event, the luminescence signal yielded by the sediment on stimulation should be a time dependant parameter. In essence, the luminescence signal intensities should decline up the depositional sequence, commensurate with decreasing age. For this assumption to be valid, however, the variations in the luminescence signal with depth should not be the result of variations induced by other parameters that influence the signal intensity within a bulk sample, apart from burial age. Such variables would include the dose rate, mineralogical concentrations, mineralogical sensitivity, sample size, as well as the degree of bleaching prior to burial. It is the consensus that aeolian dune sediments are generally well zeroed (bleached) prior to burial because the subaerial transportation they go through at the surface affords the grains adequate time for solar bleaching (e.g. Aitken, 1998; Wintle, 2008). Thus, the aeolian sequences at the Bodo site present an ideal environment for this study. To monitor changes to the dose rate so that they could be compared with the changes in the luminescence signal up the depositional section, we have measured the elemental concentrations of the responsible isotopes at given depths. Variations in the mineralogical concentrations were monitored using the IRSL/OSL signal ratios. To minimize the effect of sample size on the signal, sample portions were carefully measured aiming to produce monolayer portions. However, to test if correcting for sample size and sensitivity would make a difference, a normalization procedure was performed and used to correct the natural signals. The normalization entailed first exposing all measured portions to sunlight for at least 20 h in order to zero their signals after which a test dose of 2 Gy was then administered to each portion using a $^{137}$Cs gamma ray source at the University of Alberta. The portions were then measured again using the portable OSL reader (after preheating) and the acquired signal used to correct the natural signals. Results are provided as Supplementary data (Tables S1–S3, Figs. S1–S3) and these show that normalization did not have a major effect on the profiles. In some cases, it seemed to increase the scatter and we suspect this occurred because even though we tried to prepare portions that comprised a monolayer of sediment grains, in many cases this may have not succeeded such that multiple layers were obtained. Additionally, the grains were not fixed to the bottom of the Petri dishes that held the samples during analysis. As a result, when sample portions were transferred from the portable OSL reader to the irradiator, the sediment grains may have shifted. Such grain movement would certainly introduce scatter into the data since grains that were exposed at the surface during the initial measurement were not necessarily the same grains that were exposed after the irradiation. The only way to ascertain whether this was the source of the scatter in the normalized data would be to perform another study that binds the sediment to the base of the Petri dishes, which may be the subject of future studies. A portable OSL reader with an internal irradiator would also eliminate the need to transfer the sample from the reader to an external source. However, the portable OSL reader used in this study does not have an internal irradiation source.

An additional observation from the normalization data was that, for Sample BD03A, the data in Table S3 show that the response to the 2 Gy test dose is not uniform up the sequence. For instance, luminescence signals in the lower part (120–45 cm) following the test dose averages about 4900 counts per sample portion while the upper 40–5 cm averages about 2700 counts per portion. These differences could be the result of differences in luminescence sensitivity, possibility arising from differences in provenance for the source sediment, though the closed drainage system in the area makes this unlikely, Alternatively, it could be the result of clay or iron oxide coatings on the grain surfaces that interfere with the luminescence emissions. The upper part of the sequence was noticeably darker. Overall, however, the normalization step was not deemed to be indispensable for this study as it did not significantly alter the conclusions. Hence, the results discussed below do not include the normalized data.

### 5.1. Luminescence profiles of undisrupted depositional sequences

#### 5.1.1. Section BD01

Both the IRSL and post-IR OSL luminescence profiles obtained at Profile BD01 (Fig. 5) show very high signal intensities at the base of the profile which decrease sharply between 90 and 85 cm. From 85 cm upwards, the signal intensities fall consistently up to the surface. Variations in the feldspar content (indicated by the IRSL/OSL ratio) do not appear to account for this pattern because from 90 to 20 cm, the IRSL/OSL ratio is relatively stable. In the upper part of the sequence (20–5 cm), the feldspar content drops. This decline, however, does not appear to have an influence on the general trend of the luminescence signals because both the IRSL and post-IR OSL profiles are relatively identical. While environmental dose rates up the depositional sequence can be a factor, the concentrations of K, U and Th in BD01 are relatively constant throughout the profile such that dose rates cannot be the dominant influence shaping the luminescence profiles. This leaves burial age as the only plausible explanation for the observed patterns. If the luminescence signal intensity can be deemed directly proportional to the age of a depositional unit, luminescence signal intensities should be highest in the lower part of the stratigraphy, and lower in the upper part, which is what is observed at BD01.

The rate at which the luminescence signal decreases up the profile as well as the relative intensities of the luminescence signals provide additional information about depositional history of the sequence. For instance, the sharp fall in the luminescence signals (IRSL and post-IR OSL) observed between 90 and 85 cm (Fig. 6) indicates that the sediments at the base of the stratigraphic section are significantly older than the overlying sediments (85 cm and above), and these were most probably emplaced during an earlier period of aeolian activity. Hence, a depositional hiatus, possibly during which erosion and sediment reworking occurred, separates the older sediment (90 cm and below) from the younger sediment (85 cm and above). The more gradual decline in signal intensities from 85 to 15 cm suggests that the sediments at these depths accumulated relatively rapidly and at a constant rate (e.g. Munyikwa et al., 2012). From 10 and 5 cm, the rate of decrease in signal intensities increases slightly but this is probably due to more recent reworking at the modern surface.

Notably, neither the two bioturbated organic-rich layers between 75 and 73 cm and 70–67 cm (Fig. 5) nor the buried soil noted between 40 and 30 cm are accompanied by any significant changes in the luminescence profile as the luminescence signal appears to change uniformly in this part of the stratigraphy (Fig. 6). This suggests that the aeolian episode responsible for the rapid accumulation of sediments in the profile between 85 and 20 cm was interrupted only briefly by periods of landscape stability around 75–67 cm and around 40–30 cm. The stable periods would have been of sufficient length to allow the establishment of incipient soils, but were so brief that they do not appear as interruptions in the relative age of the samples within the luminescence profile.

Overall, the progressive decrease in luminescence signals up the depositional sequence at BD01 indicates that the depositional units at the site are stratigraphically consistent, which strongly suggests that the depositional sequence is intact, as expected, based on visual observation of the field profile.

### *5.1.2. Section BD02*

The IRSL and post-IR OSL luminescence profiles from Section BD02 (Fig. 6) demonstrate similarities with Section BD01, in that the IRSL and OSL profiles are almost indistinguishable and the signal intensities decrease up the stratigraphy. Variations in the luminescence signals cannot be explained by the variations in the IRSL/OSL ratio or by changes in the concentrations of K, U or Th, and we interpret the signal increase with depth as indicating an increase in the depositional age of the sediments.

The relatively stable luminescence signals in the lower part of the stratigraphy from 80 to 65 cm suggest a rapid accumulation of sediments, followed by the noticeable decrease in signal intensities between 65 and 60 cm indicating a depositional hiatus (and possibly a period of erosion). A subsequent gradual decrease in the luminescence signal suggests an episode of aeolian sedimentation. Again, the large decrease in photon counts between 50 and 45 cm depth suggests a depositional hiatus. In this case, the interpretation of a hiatus is supported by the presence of a buried soil between 50 and 40 cm, which indicates landscape stability (see 4.2.1; Fig. 6). Disturbance processes, including bioturbation by soil fauna and human occupation (as indicated by the artifacts recovered from this depth), would have reworked sediments at or near the stabilized land surface during this period, resulting in resetting of the luminescence signal. The gradual decrease in photon counts up the profile from 35 cm to around 10 cm suggests that this renewed sedimentation occurred relatively rapidly. A slightly steeper decline in the signal from 10 to 5 cm may be indicative of disturbances at the modern surface (Fig. 6). The soil that appears in the stratigraphy between 30 and 23 cm is not associated with a major change in the luminescence profile, suggesting that the period of landscape stability during which it developed was brief. As in Profile BD01, the luminescence profiles from BD02 point to a stratigraphic sequence that is still largely intact, as expected.

It is important to note that depositional sequences where the age difference between the youngest and oldest units is very small will return a luminescence profile that is nearly vertical. Therefore, luminescence profiling would not be capable of determining whether sediment mixing occurred in such cases. Similarly, post depositional disruption which results in thorough mixing and homogenization of the sediments will eliminate contrasts in luminescence signal intensities between the depositional units such that luminescence profiling would be ineffective. Hence, for the approach we use in this study to work, there has to be a measurable age difference between the depositional units prior to and subsequent to the mixing. Otherwise, in cases of thorough mixing, more sophisticated luminescence methods such as those that date single grains would be more appropriate (e.g. Bøtter-Jensen et al., 2000; Lamothe and Auclair, 2000).

## *5.2. Luminescence profiles of mixed depositional sequences*

As in the other two profiles examined in this study (i.e. BD01 [Fig. 5] and BD02 [Fig. 6]), the fluctuations in the luminescence signals in both stratigraphies at BD03 cannot be fully explained by either the IRSL/OSL ratio or the variations in the concentrations of K, U or Th (Figs. 8 and 9, Tables 3 and 4). This suggests that the (original) burial age of the depositional units is the main explanation for the trends noted in luminescence signal intensities. However, in contrast to the luminescence profiles at BD01 and BD02, which progressively decrease in signal intensities up the stratigraphy, the upper parts of the luminescence profiles at BD03A and BD03B appear to be inverted such that the luminescence signal rises sharply towards the surface.

At BD03A, the IRSL and post-IR OSL signals fluctuate uniformly by up to 20% between 120 and 47 cm. This fluctuation, together with the absence of a definite trend towards lower signal intensities up the depositional sequence suggests that, despite visual evidence suggesting that the lower part of the stratigraphy is intact (Fig. 8), there has been sediment mixing, interpreted here as resulting from pipeline activity which involved excavation and back-filling. The rapid decrease in the luminescence signals from 40 to 35 cm at BD03A would, under normal circumstances, denote a temporary hiatus in aeolian deposition and/or an erosional event (see examples in 5.1, above). The normalization test dose data in Table S3 pointed to the possibility of the lower part of the section having greater luminescence sensitivity, with the response to the test dose between 120 and 45 cm being close to twice higher than between 40 and 5 cm. However, this ratio would not explain the differences is signal intensities between the upper and lower parts of the section for the unnormalized data as these are up to four times greater. Hence, the proximity of Profile BD03A/B to the existing buried pipeline, and the increase in the signal intensities towards the surface confirms earlier indications from the field suggesting that the sharp contact between the lighter-coloured sands at BD03A is an artifact of backfilling procedures following pipeline-related excavations; light-coloured sands are placed back first after which the topsoil, identified on the basis of colour alone, is emplaced last. The signal intensities also suggest the dark-coloured sands were inverted during the backfilling, with sediments that used to be lower in the stratigraphy being emplaced overlying sands that were previously at the top.

Section BD03B (Fig. 9) which lies adjacent to BD03A (Fig. 8) displays luminescence profiles with signal intensities that decrease up the section but also rise sharply just below the surface, suggesting a stratigraphic inversion in the upper part of the sequence. Thus, this section too, displays signs of excavation followed by back-filling. Visually, BD03B differs from the western half of the profile (BD03A), in that signs of disturbance are evident throughout the profile, suggesting rodent burrowing and/or pipeline construction (see 4.4.1; Fig. 9). There is a general decline in the signal intensities from 120 to 60 cm which would normally indicate that the lower part of the stratigraphy is intact. However, fluctuations in both the IRSL and OSL signals around 105 and 90 cm suggest that a disruption of the original stratigraphy has occurred. The low signal intensities between 60 and 10 cm in a part of the section that appears to be visually disrupted could be explained by sediments that were exposed to sunlight at the ground surface for an extended period of time during the excavation process such that partial solar bleaching attenuated the luminescence signals. While the presence of three articulated vertebrae recovered from a depth of 60 cm might be viewed in the field as indicating that the sediments are intact, it is possible the vertebrae were excavated and reburied during the excavation process also, possibly using a large bucket, or as part of a frozen chunk of soil, and are not in their original depositional setting. Thus, overall, the luminescence profiles and stratigraphic evidence at Section BD03A and BD03B point to a depositional sequence that is not naturally intact.

## *5.3. Approximating relative ages and correlating stratigraphic profiles*

Luminescence signals collected using portable OSL readers for constructing luminescence profiles cannot readily be used to calculate absolute ages as is done in regular luminescence dating because the signals need to be calibrated. Calibration of luminescence signals is normally carried out using artificial irradiation in a lab setting to produce a growth curve that depicts the growth of the signal in the mineral grain with increasing dose. For young samples (< 30,000 years old), both quartz and feldspar show linear growth curves (e.g. Aitken, 1998). However, constructing growth curves is not a step that is necessary in luminescence profiling because we are only interested in finding out how the signal varies relatively with depth. As indicated earlier, if the dose rate, mineralogical proportions and grain size are relatively stable down the depositional sequence, the profile is a proxy for the chronostratigraphy, and the signal intensities of the individual depositional units in the profile can be deemed indicative of the relative ages of the units.

Aeolian deposits on the Northern Great Plains have been dated using both luminescence and radiocarbon methods and have been demonstrated to be of early postglacial and Holocene age (e.g. Gilliland, 2007; Wolfe et al., 2001, 2002, 2004; Munyikwa, et al., 2011). Hence, the growth curves of the luminescence signal for both quartz and feldspar would still be in the linear portion of the curve and the signal intensities up the profile can be treated as linearly proportional to the stored dose, or the sample's age. Accordingly, at Profile BD01, the OSL signal at the base of the profile (90 cm) is about 400–500% of the signal between 80 and 20 cm. Therefore, it could be argued that sediments at the base of the profile are about four to five times older than sediments between 80 and 20 cm. Similarly, at BD02, the sediments between 30 and 5 cm are about four times younger than the sediments between 80 and 65 cm. This would suggest that the difference in age between the upper and lower units in sections BD01 and BD02 is approximately the same. The normalisation step that was performed to eliminate other variables that affect the luminescence signals apart from burial time (Appendix A) showed consistency between the normalized and unnormalized data for BD01 and BD02. Hence, although preliminary, we tentatively suggest that the upper and lower units in the two profiles are correlable by their relative signal intensities. These results are consistent with luminescence dating of samples previously collected from pits at the Bodo site that was performed using regular protocols and showed that at least two major periods of aeolian deposition occurred at the site around 1700 ± 350 years ago and at 6900 ± 2300 years ago (Munyikwa et al., 2014). Hence, while the comparison made here is somewhat limited in scope, it is evident that the ability to approximate the relative ages of the depositional units using luminescence profiling imparts a quantitative context to any stratigraphic investigation.

## 6. Conclusions

Ascertaining the integrity of a site prior to conducting detailed field studies and costly excavations is an integral part of archaeological investigations, particularly with regard to HRIAs, where detailed work may add substantially to developer costs. Within this context, areas identified as previously disturbed, especially by human impact, are less valuable, and frequently require minimal further conservation, mitigation, or protection. In this study, we demonstrate that by combining detailed stratigraphic assessment and constructing luminescence profiles using the portable optically stimulated luminescence reader during HRIAs, areas that have experienced post-depositional disturbances can be rapidly and more reliably identified, even when the stratigraphic disruptions are visually indiscernible. In accordance with the basic principle of superposition of sedimentary stratigraphy, in sequences where burial age is the most important determinant of the luminescence signal, signal intensities should be higher in the lower part of the depositional sequence and decrease progressively upwards. Sequences that have experienced post-depositional mixing, on the other hand, should be characterized by a pattern attesting to the disruption of the aging-with-depth trend. Notably, however, portable OSL readers will only be useful for determining site integrity if age differences between depositional units in the sequence are significant enough to enable differentiation. Similarly, the post-depositional mixing should not be too thorough so as to produce a homogenous sequence. In such cases, more sophisticated luminescence techniques such as dating of individual grains would be more appropriate.

Thus, as a first line of approach in characterizing archaeological sites, luminescence profiling using the portable OSL reader offers a time- and cost-effective method that has unlimited application potential, including the delineation of chronological gaps in depositional sequences, identifying post-depositional disturbance, correlating depositional units across a site, and approximating relative rates of sediment accumulation. These applications are not only of use in archaeology but can be extended to geology and site investigation in forensic science applications.

## CRediT authorship contribution statement

**Kennedy Munyikwa:** Conceptualization, Methodology, Investigation, Data curation, Writing - original draft, Writing - review & editing. **Krista Gilliland:** Conceptualization, Investigation, Data curation, Writing - review & editing. **Evan Plumb:** Investigation. **Terrance Gibson:** Resources, Investigation, Data curation, Project administration.

## Acknowledgements

Gratitude is extended to Athabasca University and the Natural Science and Engineering Research Council of Canada (NSERC) for providing funding through grants to KM. Pengrowth Energy Corporation is thanked for allowing the authors to collect the data on which this work is based. Susan Fryters is thanked for proofreading several versions of this manuscript.

## Appendix A. Supplementary data

Supplementary data to this article can be found online at https://doi.org/10.1016/j.jasrep.2020.102508.

## References


Adderley, W.P., Simpson, I.A., Kirscht, H., Adam, M., Spencer, J.Q., Sanderson, D.C.W., 2004. Enhancing ethno-pedology: Integrated approaches to Kanuri and Shuwa Arab definitions in the Kala-Balge region, northeast Nigeria. Catena 58, 41–64.

Aitken, M.J., 1998. An Introduction to Optical Dating. Oxford University Press, Oxford.

Arbogast, A.F., 1996. Late Quaternary evolution of a lunette in the central Great Plains: Wilson Ridge. Kansas. Phys. Geogr. 17, 354–370.

Balee, W., 2006. The research program of historical ecology. Annual Review of Anthropology 35, 75–98.

Bayrock, L.A., 1967a. Surficial geology of the Wainwright area (east half). Alberta, Research Council of Alberta, Edmonton.

Bateman, M.D., Frederick, C.D., Jaiswal, M.K., Singhvi, A.S., 2003. Investigations into the potential effects of pedoturbation on luminescence dating. Quat. Sci. Rev. 22, 1169–1176.

Bateman, M.D., Boulter, C.H., Carr, A.S., Frederick, D.D., Peter, D., Wilder, M., 2007. Preserving the palaeoenvironmental record in drylands: Bioturbation and its significance for luminescence –derived chronologies. Sediment. Geol. 195, 5–19.

Bateman, M.D., Stein, S., Ashurst, R.A., Selby, K., 2015. Instant luminescence chronologies? High resolution luminescence profiles using a portable luminescence reader. Quat. Geochronol. 30, 141–146.

Bateman, M.D., Rushby, G., Stein, S., Ashurst, R.A., Stevenson, D., Jones, J.M., Gehrels, W.R., 2018. Can sand dunes be used to study historic storm events? Earth Surf. Procesess. Landf. 43, 779–790.

Bayrock, L.A., 1967b. Surficial geology of the Wainright area (east half), Alberta. Res. Council of Alberta, Report 67–74.

Becerra-Valdivia, L., Higham, T., 2020. The timing and effect of the earliest human arrivals in North America. Nature. https://doi.org/10.1038/s41586-020-2491-6.

Blaikie, K., 2005. Archaeological Investigations of FaOm-1: The Bodo Bison Skulls Site. Unpublished Master's thesis. Department of Anthropology, University of Alberta, Edmonton.

Blott, S.J., Pye, K., 2006. Particle size distribution analysis of sand-sized particles by laser diffraction: an experimental investigation of instrument sensitivity and the effects of particle shape. Sedimentology 53, 671–685.

Blott, S.J., Pye, K., 2001. GRADISTAT: A grain size distribution and statistics package for the analysis of unconsolidated sediments. Earth Surf. Process. Landf. 26, 1237–1248.

Bøtter-Jensen, L., 2000. Luminescence techniques using natural minerals and ceramics and their application to retrospective dosimetry. Unpublished PhD thesis. University of Copenhagen, Denmark.

Bøtter-Jensen, L., Bulur, E., Duller, G.A.T., Murray, A.S., 2000. Advances in luminescence instrument systems. Radiat. Meas. 32, 523–528.

Boulter, C., Bateman, M.D., Frederick, C.D., 2010. Understanding geomorphic responses

to environmental change: A 19 000-year case study from semi-arid central Texas. USA. J. Quat. Sci. 25, 889–902.
Bubel, S., 2014. The fincastle site: A late middle prehistoric bison kill on the Northwestern Plains. Plains Anthropol. 59, 207–240.
Crumley, C.L., 1994. Historical ecology. In: Crumley, C.L. (Ed.), Historical ecology: cultural knowledge and changing landscapes. School of American Research Press, Santa Fe, pp. 1–16.
David, P.P., 1977. Sand dune occurrences of Canada: a theme and resource inventory study of Aeolian landforms of Canada. DIAND, National Parks Branch, Ottawa Contract No. 74–230, 183 pp.
Day, J., H.,, 1983. Canada Soil Information system (CanSIS) manual for describing soils in the field. Research Branch, Agriculture Canada, Ottawa.
Dyck, I., Morlan, R.E., 1995. The Sjovold Site. A river crossing campsite in the Northern Plains, Canadian Museum of Civilization, Hull.
Feathers, J.K., 2003a. Use of luminescence dating in archaeology. Meas. Sci. Technol. 14, 1493–1509.
Feathers, J.K., 2003b. Single-grain OSL dating of sediments from the Southern High Plains. USA. Quat. Sci. Rev. 22, 1035–1042.
Folk, R.L., Ward, W.C., 1957. Brazos river bar: a study of significance of grain size parameters. J. Sediment. Petrol. 27, 3–26.
Forman, S.L., Oglesby, R., Webb, R.S., 2001. Temporal and spatial patterns of Holocene dune activity on the Great plains of North America: megadroughts and climate links. Global Planet. Change 29, 1–29.
Frison, G.C. (Ed.), 2013. The Casper site: A Hell Gap Bison Kill on the high Plains, revised ed. Pecheron Press, Clinton Corners, New York.
Geobel, T., Waters, M.R., O'Rourke, D.H., 2008. The Late Pleistocene dispersal of modern humans in the Americas. Science 319, 1497–1501.
Ghilardi, M., Sanderson, D., Kinnaird, T., Bicket, A., Balossino, S., Parisot, J.-C., Hermitte, D., Guibal, F., Fleury, J.T., 2015. Dating the bridge at Avignon (south France) and reconstructing the Rhone River fluvial palaeo-landscape in Provence from medieval to modern times. J. Archaeol. Sci. Rep. 4, 336–354.
Gibson, T., Grekul, C., 2010. Excavation of a campsite living floor at PL1 in the Bodo Archaeological Locality, Final report. Archaeological research permit 2001-284. On file at Alberta Culture, Edmonton.
Gibson, T., McKeand, P., 1996. Heritage Resources Impact Assessment of a Fletcher Challenge Petroleum Pipeline in the Eyehill Creek Locality, Bodo, Alberta. Archaeological research permit no. 95–101 Report on file at Alberta Community Development, Edmonton.
Gilliland, K., 2007. Geoarchaeology of the Bodo Archaeological Locality, Alberta. Unpublished Master's thesis. Department of Anthropology, University of Alberta, Edmonton.
Gilliland, K., 2012. Historical resources impact assessment prior to liner insertion program at FaOm-1, the Bodo Archaeological Locality, Alberta, Final report. Archaeological research permit no. 12-159. Report on file at Alberta Culture, Edmonton.
Gray, H.J., Mahan, S.A., Springer, K.B., Pigati, J.S., 2018. Examining the relationship between portable luminescence reader measurements and depositional ages of paleowetland sediments, Las Vegas Valley. Nevada. Quat. Geochronol. 48, 80–90.
Gray, H.J., Jain, M., Sawakuchi, A.O., Mahan, S.A., Tucker, G.E., 2019. Luminescence as a sediment tracer and provenance tool. Rev. Geophys. https://doi.org/10.1029/2019RG000646.
Grekul, C., 2007. A Zooarchaeological Analysis of a Late Precontact Bison Kill Site in the Bodo Sand Hills of Alberta. Unpublished Master's thesis. Department of Anthropology, University of Alberta, Edmonton.
Halfen, A.F., Lancaster, N., Wolfe, S., 2015. Interpretations and common challenges of aeolian records from North American dune fields. Quat. Int. 410, 75–95.
Hall, S.A., Goble, R.J., Paleosol, Berino, 2012. Late Pleistocene argillic soil development on the Mescalero Sand Sheet in New Mexico. J. Geol. 120, 333–345.
Hall, S.A., Miller, M.R., Goble, R.J., 2010. Geochronology of the Bolson sand sheet, New Mexico and Texas, and its archaeological significance. Geol. Soc. Am. Bull. 122, 1950–1967.
Hall, S.A., Goble, R.J., 2008. Archaeological geology of the Mescalero Sands Southeastern New Mexico. Plains Anthropol. 53, 279–290.
Hamilton, S., Nicholson, B.A., 1999. Ecological islands and Vickers Focus adaptive transitions in the pre-contact Plain in southwestern Manitoba. Plains Anthropol. 44, 5–25.
Hetherington, R., Barrie, V.J., MacLeod, R., Wilson, M., 2004. Quest for lost land. Geotimes 49, 20–23.
Holen, S, 1990. Anthropology: The Native American Occupation of the Sand Hills. In A. Bleed, and C. Flowerday (Eds). An Atlas of the Sand Hills (pp. 189-205). University of Nebraska Conservation and Survey Division Resource Atlas 5a. University of Nebraska-Lincoln.
Holliday, V.T., 2000a. The evolution of Paleoindian Geochronology and Typology on the Great Plains. Geoarchaeology 15, 227–290.
Holliday, V., 2000b. Folsom Drought and Episodic Drying on the Southern High Plains from 10,900–10,200 14C yr B.P. Quat. Res. 53, 1–12.
Holliday, V.T., 2001. Stratigraphy and geochronology of upper Quaternary eolian sand on the southern high plains of Texas and New Mexico. Geol. Soc. Am. Bull. 113, 88–108.
Hopkins, D.G., Running, G.L., 2000. Soils, Dunes, and Prairie Vegetation: Lessons from the Sandhills of North Dakota. In: Radenbaugh, T.A., Douaud, P.C. (Eds.), Changing prairie landscapes. Canadian Plains Research Center, University of Regina, Regina, pp. 39–57.
Jain, M., Singhvi, A.K., 2001. Limits to depletion of blue-green light stimulated luminescence in feldspars: Implications for quartz dating. Radiat. Meas. 33, 883–892.
Kinnaird, T.C., Sanderson, D.C.W., Woodward, N.L., 2012. Applying luminescence methods to geoarchaeology: A case study from Stronsay, Orkney. Earth Env. Sci. Tran. Roy. Soc. Edin. 102, 191–200.
Kinnaird, T.C., Sanderson, D.C.W., Bigelow, G.F., 2015. Feldspar SARA IRSL dating of very low dose rate eolian sediments from Sandwick South, Unst. Sheltand. Quat. Geochronol. 30, 168–174.
Kinnaird, T., Bolos, J., Turner, A., Turner, S., 2017. Optically-stimulated luminescence profiling and dating of historic agricultural terraces in Catalonia (Spain). J. Archaeol. Sci. 78, 66–77.
Lamothe, M., Auclair, M., 2000. The fadia method: A new approach in luminescence dating using the analysis of single feldspar grains. Radiat. Meas. 32, 433–438.
Lian, O.B., Roberts, R.G., 2006. Dating the Quaternary: Progress in luminescence dating of sediments. Quat. Sci. Rev. 25, 2449–2468.
Leigh, D.S., 2001. Buried artifacts in sandy soils: techniques for evaluating pedoturbation versus sedimentation. In: Goldberg, P., Holliday, V., Reid Ferring, C. (Eds.), Earth Science and Archaeology. Kluwer Academic / Plenum Publishers, New York, pp. 269–293.
McKeague, J.A., 1981. Manual on soil sampling and methods of analysis, 2nd ed. Canadian Society of Soil Science, Ottawa, Prepared by the Subcommittee on methods of analysis.
Mills, C., Simpson, I., Adderley, P., 2014. The lead legacy: the relationship between historical mining, pollution and the post-mining landscape. Landsc. Hist. 35, 47–72.
Montenegro, A., Hetherington, R., Eby, M., Weaver, A.J., 2006. Modelling pre-historic crossings into the Americas. Quat. Sci. Rev. 25, 1323–1338.
Muhs, D.R., Wolfe, S.A., 1999. Sand dunes of the northern Great Plains of Canada and the United States. In: Lemmen, D.S., Vance, R.E. (Eds.), Holocene Climate and Environmental Change in the Palliser Triangle: a geoscientific context for evaluating the impacts of climate change on the southern Canadian Prairies. Geological Survey of Canada, Ottawa, pp. 183–197.
Muhs, D.R., Holliday, V.T., 2001. Origin of Late Quaternary dune fields on the southern High plains of Texas and New Mexico. Geol. Soc. Am. Bull. 113, 75–87.
Mulira, J.E., 1986. Eolian Landforms of Alberta, Alberta Forestry. Resource Evaluation and Planning and Public Lands Divisions, Edmonton, Lands and Wildlife.
Munyikwa, K., Feathers, J.K., Rittenour, T.M., Shrimpton, H.K., 2011. Constraining the Late Winsconsinan retreat of the Laurentide ice sheet from western Canada using luminescence ages from postglacial aeolian dunes. Quat. Geochronol. 6, 407–422.
Munyikwa, K., Brown, S.T., Kitabwalla, Z., 2012. Delineating stratigraphic breaks at the bases of postglacial eolian dunes in central Alberta, Canada using a portable OSL reader. Earth Surf. Process. Landf. 37, 1603–1604.
Munyikwa, K., Brown, S., 2014. Rapid equivalent dose estimation for eolian dune sands using a portable OSL reader and polymineralic standardised luminescence growth curves: Expedited sample screening for OSL dating. Quat. Geochronol. 22, 116–125.
Munyikwa, K., Gilliland, K., Gibson, T., Mann, E., Rittenour, T.M., Grekul, C., Blaikie-Birkigt, K., 2014. Late Holocene temporal constraints for human occupation levels at the Bodo archaeological locality, east central Alberta, Canada using radiocarbon and luminescence chronology. Plains Anthropol. 59, 109–143.
Munyikwa, K., Ritennour, T., Feathers, J.K., 2017. Temporal constraints for the Late Wisconsinan deglaciation of western Canada using eolian luminescence chronologies from Alberta. Palaeogeogr. Palaeoclimatol. Palaeoecol. 470, 147–165.
Munyikwa, K., Lindemann, R., Wondrasek, R., Kinnaird, T.C., Sanderson, D.C.W., 2019. Temporal constraints for Holocene geomorphic evolution at an archaeological locality near Hardisty, east-central Alberta: Hunter Gatherer Interactions with the Landscape on the northern Plains. Can. J. Archaeol. 43, 40–73.
Muñoz-Salinas, E., Bishop, P., Sanderson, D.C.W., Zamorano, J.J., 2011. Interpreting luminescence data from a portable OSL reader: Three case studies in fluvial settings. Earth Surf. Process. Landf. 36, 651–660.
Muñoz-Salinas, E., Bishop, P., Sanderson, D., Kinnaird, T., 2014. Using OSL to assess hypothesis related to the impacts of land use change with the early nineteenth century arrival of Europeans in south-eastern Australia: An exploratory case study from Grabben Gullen Creek, New South Wales. Earth Surf. Process. Landf. 39, 1576–1586.
Murray, A.S., Wintle, A.G., 2003. The single portion regenerative dose protocol: Potential for improvements in reliability. Radiat. Meas. 37, 377–381.
Neuman, R.W., 1967. Radiocarbon dated archaeological remains on the Northern and Central Great Plains. Am. Antiq. 32, 471–486.
Porat, N., Lopez, G.I., Lensky, N., Elinson, R., Avni, Y., Elgart-Sharon, Y., Faershtein, G., Gadot, Y., 2019. Using a portable OSL reader to obtain a time scale for soil accumulation and erosion in archaeological terraces, the Judean Highlands. Israel. Quat. Geochronol. 49, 65–70.
Portenga, E.W., Bishop, P., 2016. Confirming geomorphological interpretations based on portable OSL reader data. Earth Surf. Process. Landf. 41, 427–432.
Portenga, E.W., Bishop, P., Gore, D.B., Westway, K.E., 2016. Landscape preservation under post-European settlement alluvium in the south-eastern Australian tablelands, inferred from portable OSL reader data. Earth Surf. Process. Landf. 41, 1697–1707.
Potter, B.A., Baichtal, J.F., Beaudoin, A.B., Fehren-Schmitz, L., Haynes, C.V., Holliday, V.T., Holmes, C.E., Ives, J.W., Kelly, R.L., Llamas, B., Malhi, R.S., Miller, S.D., Reich, D., Reuther, J.D., Schiffels, S., Surovell, T.A., 2018. Current evidence allows multiple models for the peopling of the Americas. Sci. Adv. 4 eaat5473.
Prescott, J.R., Hutton, J.T., 1988. Cosmic-ray and gamma ray dosimetry for TL and electron-spin-resonance. Nucl. Tracks Radiat. Meas. 14, 223–227.
Preston, J., Sanderson, D., Kinnaird, T., Newton, A., Nitter, M., Coolen, J., Mehler, N., Dugmore, A., 2019. Dynamic beach response to changing storminess of Unst, Shetland: implications for landing places exploited by Norse communities. J. Island Coast. Archaeol. https://doi.org/10.1080/15564894.2018.1555193.
Roberts, R.G., 1997. Luminescence dating in archaeology: From origins to optical. Radiat. Meas. 27, 819–892.
Roberts, R.G., Galbraith, R.F., Yoshida, H., Laslett, G.M., Olley, J.M., 2000. Distinguishing dose populations in sediment mixtures: A test of single-grain optical dating procedures using mixtures of laboratory dosed quartz. Radiat. Meas. 32, 459–465.

Roberts, H.M., Wintle, A.G., 2001. Equivalent dose determinations for polymineralic fine-grains using the SAR protocol: Applications to a Holocene sequence of the Chinese Loess Plateau. Quat. Sci. Rev. 20, 859–863.
Rother, H., Lorenz, S., Börner, A., Kenzler, M., Siermann, N., Fülling, A., Hrynowiecka, A., Forler, A., Kuznetsov, Maksimov F., Starikova, A., 2019. The terrestrial Eemian to late Weichselian sediment record at Beckentin (NE-Germany): First results from lithostratigraphic, palynological and geochronological analyses. Quat. Int. 501, 90–108.
Running, G.L., Havholm, K., Boyd, M., Wiseman, D., 2002. Holocene stratigraphy and geomorphology of Flintstone Hill, Lauder Sandhills, Glacial Lake Hind Basin, southwestern Manitoba Canada. Geogr. Phys. Quat. 56, 291–303.
Sanderson, D.C.W., Murphy, S., 2010. Using simple portable measurements and laboratory characterisation to help understand complex and heterogeneous sediment sequences for luminescence dating. Quat. Geochronol. 5, 299–305.
Shetsen, I., 1990. Quaternary Geology Central Alberta, Alberta Research Council Natural Resources Division. Terrain Sci. Department, Edmonton. 1 (500), 000.
Stauch, G., 2019. A conceptual model for the interpretation of aeolian sediment from a seimarid high-mountain environment since the late Glacial. Quat. Res. 91, 24–34.
Stone, A.E.C., Bateman, M.D., Thomas, D.S.G., 2015. Rapid age assessment in the Namib Sand Sea using a portable luminescence reader. Quat. Geochronol. 30, 134–140.
Stone, A., Bateman, M.D., Burrough, S.L., Garzanti, E., Limonta, M., Radeff, G., Telfer, M.W., 2019. Using a portable luminescence reader for rapid age assessment of aeolian sediment for reconstructing dunefield landscape evolution in southern Africa. Quat. Geochronol. 49, 57–64.
Thompsen, K.J., Jain, M., Murray, A.S., Denby, P.M., Roy., N., Bøtter-Jensen,, 2008. Minimizing feldspar OSL contamination in quartz UV-OSL using pulsed blue stimulation. Radiat. Meas. 43, 752–757.
Vickers, J.R., 1986. Alberta Plains Prehistory: A review. Alberta Culture, Edmonton.
Wallinga, J., Murray, A.S., Bøtter-Jensen, L., 2002. Measurement of the dose in quartz in the presence of feldspar contamination. Radiat. Prot. Dosim. 101, 367–370.
Waters, M.R., Stafford Jr., T.W., 2007. Redefining the age of Clovis: Implications for the peopling of the Americas. Science 315, 1122–1126.
Wettlaufer, B.N., 1955. The Mortlach Site in the Besant Valley of Central Saskatchewan. Department of Natural Resources, Regina.
Wintle, A.G., 2008. Luminescence Dating: Where it has been and where it is going. Boreas 37, 471–482.
Wolfe, S.A., Huntley, D.J., David, P.P., Ollerhead, J., Sauchyn, D.J., MacDonald, G.M., 2001. Late 18$^{th}$ century drought-induced sand dune activity, Great Sand Hills Saskatchewan. Can. J. Earth Sci. 38, 105–117.
Wolfe, S.A., Ollerhead, J., Huntley, D.J., Campbell, C., 2002. Late Holocene dune activity in the Duchess dune field, Alberta Geological Survey of Canada, Ottawa. Curr. Res. 2002–B3.
Wolfe, S.A., Huntley, D.J., Ollerhead, J., 2004. Relict Late Wisconsinan dune fields of the northern Great Plains. Canada. Geogr. phys. Quat. 58, 323–336.
Wolfe, S.A., Hugenholtz, C.H., Evans, C.P., 2007. Potential aboriginal-occupation-induced dune activity, Elbow Sand Hills, northern Great Plains Canada. Great Plains Res. 17, 173–192.
Wood, W.R., 1998. Archaeology on the Great Plains. University Press of Kansas, Lawrence.